Raytheon

60 GHz Solid State Power Amplifier

FINAL TECHNICAL REPORT

March 1, 1991
RAY/RD/S-4580

Prepared for
National Aeronautics and Space Administration
Goddard Space Flight Center
Greenbelt Road
Greenbelt, MD 20771

Prepared by
Raytheon Company
Research Division
131 Spring Street
Lexington, Massachusetts 02173

NASA
National Aeronautics and Space Administration

Report Documentation Page

1. Report No.	2. Government Accession No.	3. Recipient's Catalog No.

4. Title and Subtitle

60 GHz Solid State Power Amplifier

5. Report Date

03/01/91

6. Performing Organization Code

7. Author(s)

J. McClymonds

8. Performing Organization Report No.

10. Work Unit No.

9. Performing Organization Name and Address

Raytheon Company
Research Division
131 Spring Street
Lexington, MA 02173

11. Contract or Grant No.

NASS-30356

13. Type of Report and Period Covered

Final Technical

12. Sponsoring Agency Name and Address

National Aeronautics and Space Administration
Goddard Space Flight Center
Greenbelt Road, Greenbelt, MD 20771

14. Sponsoring Agency Code

15. Supplementary Notes

16. Abstract

A new amplifier architecture was developed during this contract that is superior to any other solid state approach. The amplifier produced 6 watts with 4 percent efficiency over a 2 GHz band at 61.5 GHz. The unit was 7 x 9 x 3 inches in size, 5.5 pounds in weight, and the conduction cooling through the baseplate is suitable for use in space.

The amplifier used high efficiency GaAs IMPATT diodes which were mounted in 1-diode circuits, called modules. Eighteen modules were used in the design, and power combining was accomplished with a proprietary passive component called a combiner plate.

17. Key Words (Suggested by Author(s))	18. Distribution Statement
Solid state amplifier, V-band amplifier, IMPATT diodes, IMPATT diode amplifier, Power combining	

19. Security Classif. (of this report)	20. Security Classif. (of this page)	21. No. of pages	22. Price
Unclassified	Unclassified	63	

NASA FORM 1626 OCT 86

RAYTHEON COMPANY
Research Division
131 Spring Street
Lexington, MA 02173

60 GHZ SOLID STATE POWER AMPLIFIER

NAS5-30356

Final Technical Report

RAY/RD/S-4580

March 1, 1991

Prepared for

National Aeronautics and Space Administration
Goddard Space Flight Center
Greenbelt Road
Greenbelt, MD 20771

TABLE OF CONTENTS

Section		Page
1.0	INTRODUCTION	1-1
	1.1 Design Overview	1-2
2.0	AMPLIFIER COMPONENTS	2-1
	2.1 GaAs IMPATT Diodes	2-1
	2.2 IMPATT Circuits	2-3
	2.3 Combiner Plate	2-19
	2.4 Isolator/Circulator Assemblies	2-25
	2.5 Electronic Circuits	2-27
	2.6 Thermal Design	2-34
3.0	AMPLIFIER ASSEMBLY AND TEST RESULTS	3-1
	3.1 Amplifier Assembly and Output Power Measurements	3-1
	3.2 Measurement of Spurious Signals	3-5
	3.3 Burn-In	3-6
4.0	RELIABILITY PREDICTION	4-1
5.1	CONCLUSIONS	5-1

LIST OF ILLUSTRATIONS

Figure No.		Page
1-1	Block Diagram of NASA Amplifier	1-3
1-2	Photograph of the Amplifier Removed from the Chassis	1-4
1-3	Photograph of the Amplifier with the Cover Removed	1-6
1-4	Photograph of the Amplifier with the Cover Installed	1-7
2-1	Photograph of a "Cut-Away" 60 GHz IMPATT Diode	2-2
2-2	Photograph of the High Power 60 GHz Network Analyzer	2-4
2-3	Cross Section of the First Prototype 60 GHz IMPATT Amplifier Module	2-5
2-4	Photograph of the First Prototype IMPATT Amplifier Module	2-6
2-5	Circuit Impedance Measurements of the First Prototype IMPATT Module Using Three Different Waveguide Transformers	2-7
2-6	Active and Passive Impedance Data from the First Prototype IMPATT Module	2-10
2-7	Cross Section of the Second Prototype IMPATT Amplifier Module	2-13
2-8	Photograph of the Second Prototype IMPATT Amplifier Module	2-14
2-9	Circuit Impedance of the Second Prototype IMPATT Module with the Coaxial Spacer Removal	2-15
2-10	Circuit Impedance of the Second Prototype IMPATT Module with Two Different Coaxial Spacers	2-16
2-11	Polar Plot of the Device and Circuit Impedances of the Second Prototype IMPATT Module	2-17
2-12	Output Power of the Second Prototype IMPATT Module	2-18
2-13	Photograph of Assembled and Disassembled IMPATT Modules used to Construct the Amplifier	2-20

LIST OF ILLUSTRATIONS

Figure No.		Page
2-14	Insertion Loss of the 8-Way Combiner Network in the Combiner Plate	2-21
2-15	Input Match of the Three Combiner Networks in the Combiner Plate	2-22
2-16	Transmission Loss of an Aluminum Waveguide (upper graph)	2-24
2-17	Photograph of a 1-Junction Circulator and a 2-Junction Circulator	2-26
2-18	Simplified Schematic of the Bias Regulator Circuit	2-28
2-19	Photograph of a Bias Regulator Circuit Board	2-29
2-20	Performance of the Bias Regulator Circuit	2-31
2-21	Block Diagram of the Control Circuit	2-32
2-22	Photograph of the Control Board	2-33
2-23	Front View of the Amplifier Chassis	2-35
2-24	Rear View of the Amplifier Chassis	2-36
3-1	Performance of the Seven Stages in the Amplifier	3-3
3-2	Output Power of the Amplifier	3-7
4-1	Reliability Data of GaAs IMPATT Diodes	4-2

LIST OF TABLES

Table No.		Page
3-1	Spreadsheet Analysis of the 7-Stage Amplifier Design	3-2

1.0 INTRODUCTION

Amplifiers at 60 GHz will have an important role for communication between satellites or between a satellite and a space shuttle. Very high gain antennas can be constructed because the wavelength is so short, reducing the amplifier power requirement. Also, the communication links will be secure, because the 60 GHz signals will be totally absorbed in the atmosphere before reaching the ground.

New technologies were developed in this NASA contract for a high efficiency solid state amplifier at 60 GHz. The goals and achieved results are listed below.

Contract Goals

Center Frequency	61.5 GHz
Bandwidth	2 GHz
Output Power	10 Watts
Gain	40 dB
Efficiency	10 Percent
Spurious Output	-30 dBc (maximum)
Cooling	Suitable for spacecraft
Reliability	100,000 hours (calculation)
Weight	As light as possible
Size	As small as possible

Achieved Results

Center Frequency	61.5 GHz
Bandwidth	2 GHz
Output Power	5.9 to 6.5 Watts
Gain	40 dB
Efficiency	3.8 to 4.2 Percent
Spurious Output	-30 dBc (maximum)
Cooling	Conduction through baseplate
Reliability	200,000 hours (calculation)
Weight	5.5 pounds
Size (not including air cooling components)	7" x 8.8" x 3" (significant further reduction feasible)

1.1 Design Overview

The active devices that are used in this amplifier are Raytheon GaAs double-drift IMPATT diodes. In general, an IMPATT diode is the solid-state device with the highest power at millimeter-wave frequencies, and GaAs double-drift IMPATTs have the best combination of power and efficiency. These devices have been under development for several years through contracts from the Air Force Space Technology Center, and the Air force Wright Avionics Laboratory.

The architecture which is used to build this amplifier is based on IMPATT circuits, or modules, each containing one active device. Figure 1-1 illustrates that the first three stages have one high gain module apiece, providing a total gain of approximately 28 dB. The last four stages use modules that are optimized for high power at lower gain, and the number of modules per stage is doubled at each step. The gain of these last four stages is approximately 3 dB, so the number of diodes in these stages is proportional to the added power required by the stage.

Power combining in the multiple diode stages is performed with a proprietary combiner plate. This is a passive component which sums the outputs of all the modules in a stage with negligible attenuation. RF power is channeled from one stage to another through waveguide sections and isolator/circulator assemblies. The amplifier also contains the necessary electronics to supply bias current to each diode.

Figure 1-2 is a photograph of the amplifier. The combiner plate is the thick plate at the bottom of the amplifier, and the IMPATT modules are the small metal cubes on the upper surface of the combiner plate. The narrow circuit board attached to each module is a bias regulator circuit. They are connected to the control board at the rear of the unit through a wiring harness. Over one-half of the amplifier volume is consumed by the bias

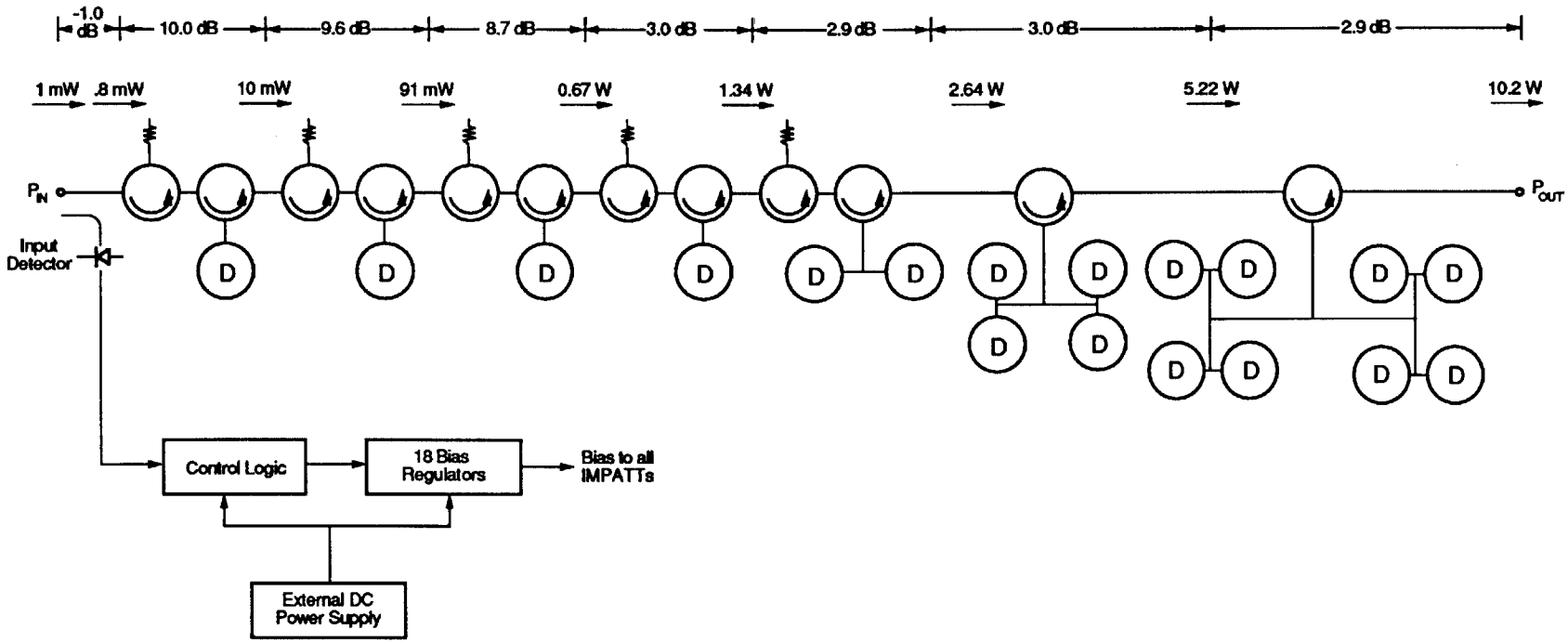

Figure 1-1. Block Diagram of NASA Amplifier.

ORIGINAL PAGE
BLACK AND WHITE PHOTOGRAPH

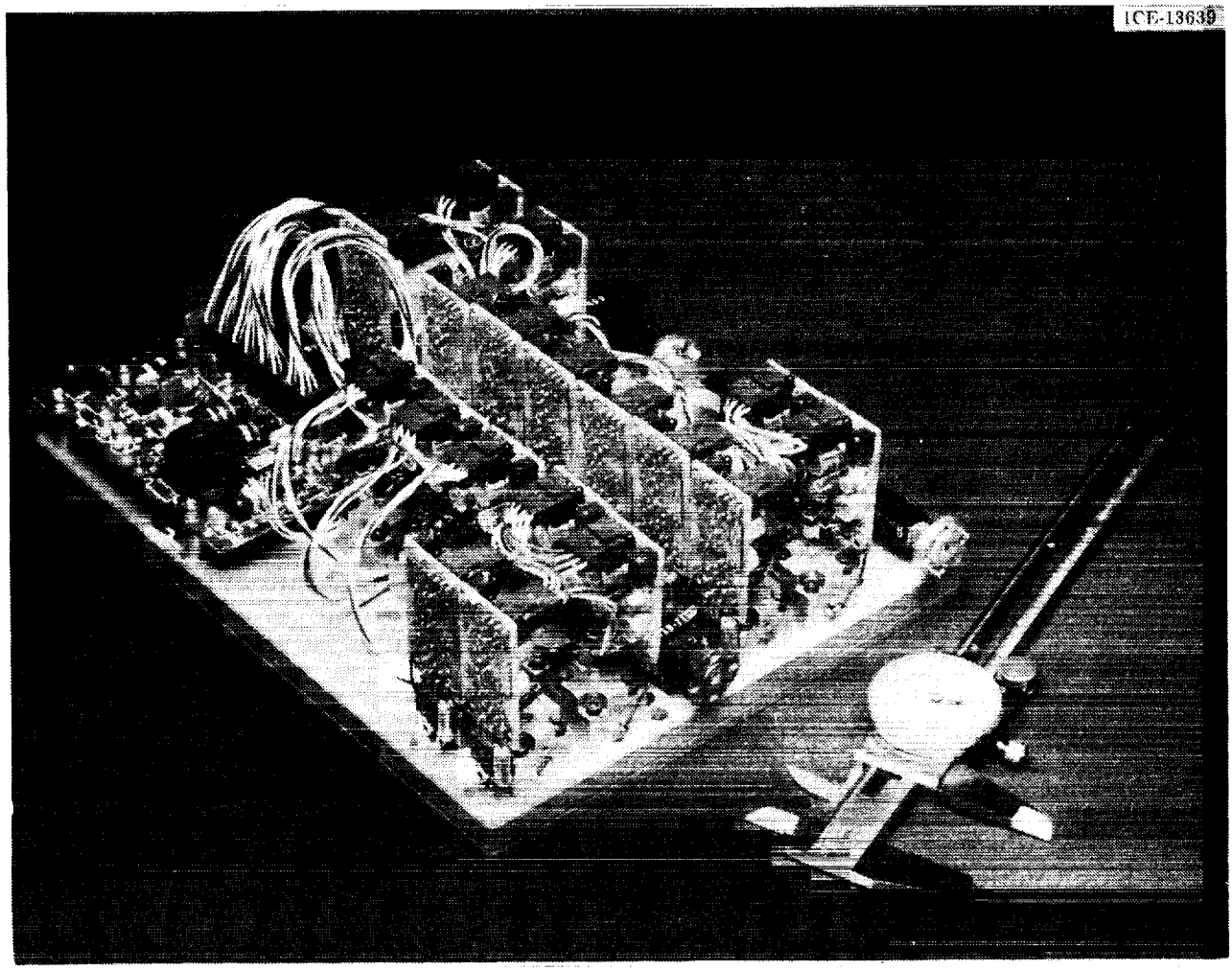

Figure 1-2. Photograph of the Amplifier Removed from the Chassis.

regulator circuit boards which extend well above any other component. In the future, the bias regulators could be constructed as hybrid circuits, significantly reducing the amplifier size.

The amplifier is conduction cooled through the bottom of the combiner plate, which is appropriate for a space application. An air cooled heat exchanger was built in order that this prototype amplifier could be easily operated in the laboratory. Figure 1-3 is a photograph of the amplifier when it is installed on this heat exchanger. The cooling fins are visible through the opening in the front panel, and a small "muffin" fan is located in the plenum at the rear of the amplifier. Figure 1-4 shows the completed amplifier with the cover attached.

The remainder of this final report is divided into four sections. Section 2 describes the design and performance of the RF, electronic and thermal components. Section 3 discusses the assembly of the amplifier and the test results. Section 4 shows the results of a reliability analysis, and Section 5 concludes with recommendations for further development of solid-state amplifiers.

ORIGINAL PAGE
BLACK AND WHITE PHOTOGRAPH

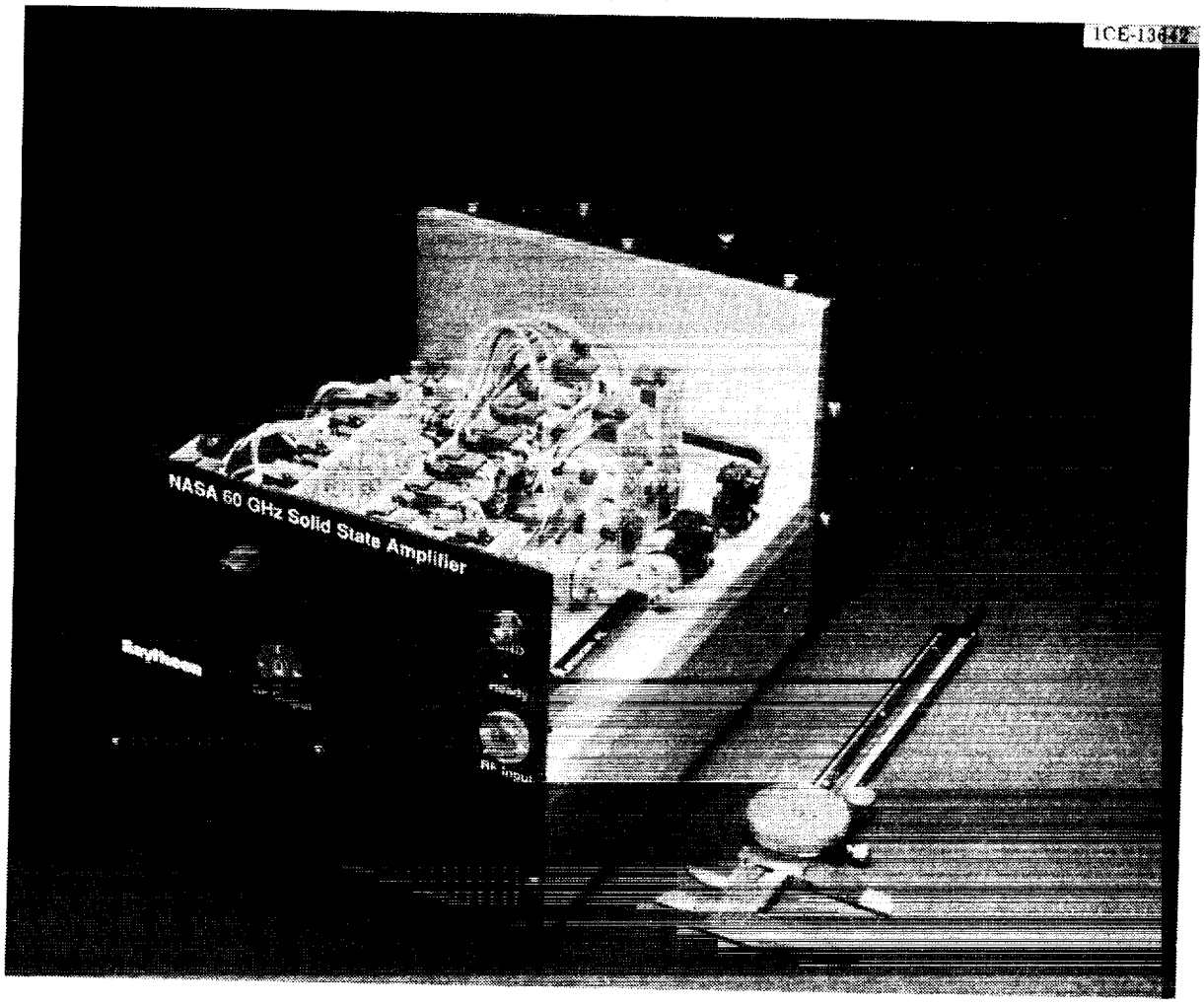

Figure 1-3. Photograph of the Amplifier with the Cover Removed.

ORIGINAL PAGE
BLACK AND WHITE PHOTOGRAPH

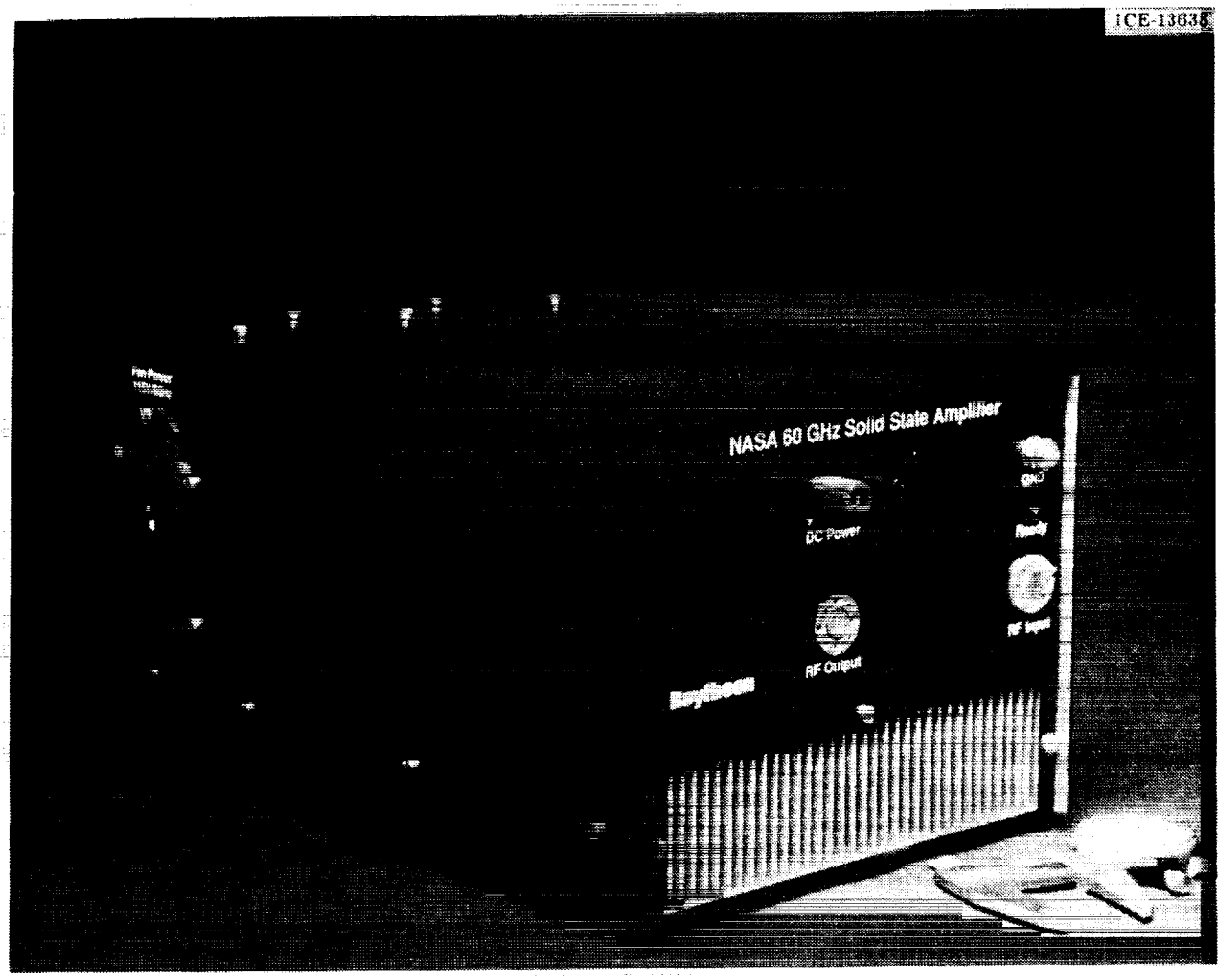

Figure 1-4. Photograph of the Amplifier with the Cover Installed.

2.0 AMPLIFIER COMPONENTS

In developing the component set for this contract, we used the design philosophy of "screw it together and turn it on." If this goal is achieved, all the components can be tuned to specification individually and they will operate together in the final assembly without readjustment. This will ensure that each component is delivering its optimum performance, and the assembly procedure is greatly simplified.

Implementing this philosophy for a millimeter-wave amplifier requires careful design and control of the RF and electrical interfaces. We chose to use a matched load as the RF interface convention, which means that all waveguide ports on the passive components must have a very good match and accurate mechanical alignment. Thus, when components are connected together in the final assembly, one device does not load pull another. Similarly, the electronic circuits were designed so that they cannot interfere with each other. This philosophy was successfully implemented in the design of this amplifier. The remainder of this section will describe the design and performance of each major component.

2.1 GaAs IMPATT Diodes

The Raytheon GaAs IMPATT diodes that are used in this amplifier have the following typical properties.

Typical IMPATT Diode Performance

Power:	1.0 watts
Efficiency:	11 percent
ΔT_j:	170°C

The power and efficiency of these devices set the state of the art at this frequency. Figure 2-1 is a photograph of a packaged

ORIGINAL PAGE
BLACK AND WHITE PHOTOGRAPH

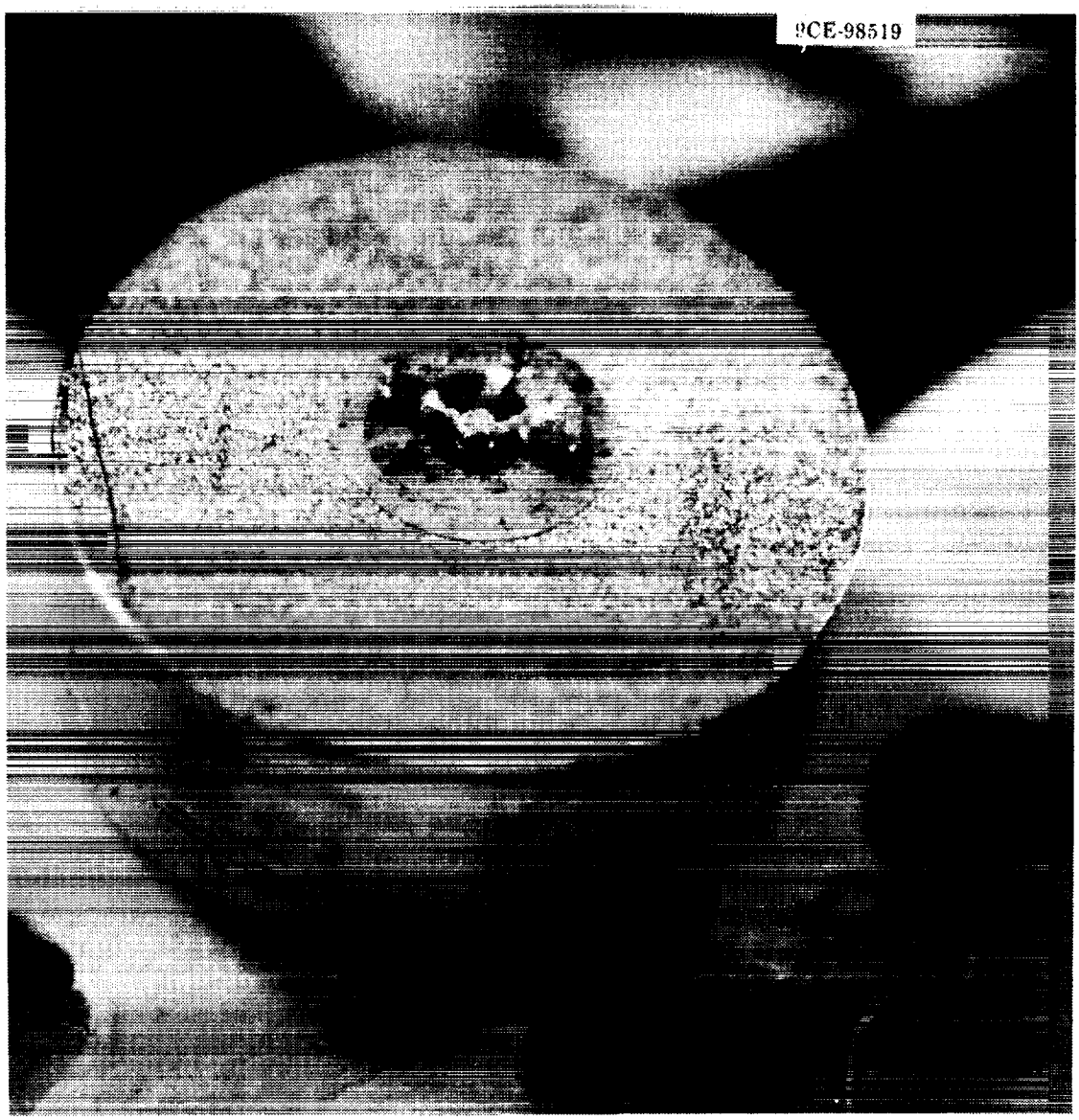

Figure 2-1. Photograph of a "Cut-Away" 60 GHz IMPATT Diode.

diode that has half of the ceramic insulator removed. A 0.030-inch diameter diamond has been pressed into a 0.116-inch diameter copper puck to form a high thermal conductivity heatsink. The ceramic insulator and the single-mesa IMPATT chip are thermal-compression bonded to the metalized diamond surface. The four integral beam leads connect the top contact of the mesa to the top of the ceramic insulator. A cap that is the same diameter as the insulator is soldered in place to mechanically protect the diode and provide a hermetic enclosure. The overall yield of our diodes, including the dc burn-in and RF evaluation is about 30 percent, which is quite high for such a complex device.

The IMPATT chips which we used to fabricate diodes for this amplifier have a relatively small junction area. Larger devices produce approximately 1.5 watts, but this amplifier design only required 1.0 watt devices. The efficiency of the larger devices is considerably poorer at the 1 watt bias level, and the smaller devices were optimized for this application.

2.2 IMPATT Circuits

An IMPATT diode is a low impedance, high current device. Therefore, IMPATTs must be operated in a special circuit which transforms the high impedance of the output waveguide to a level which is appropriate to match the diode. The greatest technical challenge of this contract was to develop an IMPATT module which had the correct gain across the operating band and low attenuation.

Our first task in the development of the IMPATT circuit was to design and build a high power automatic network analyzer. This would allow us to completely analyze the passive amplifier circuits and measure the characteristics of the IMPATT diodes under actual operating conditions. Figure 2-2 is a photograph of this

ORIGINAL PAGE
BLACK AND WHITE PHOTOGRAPH

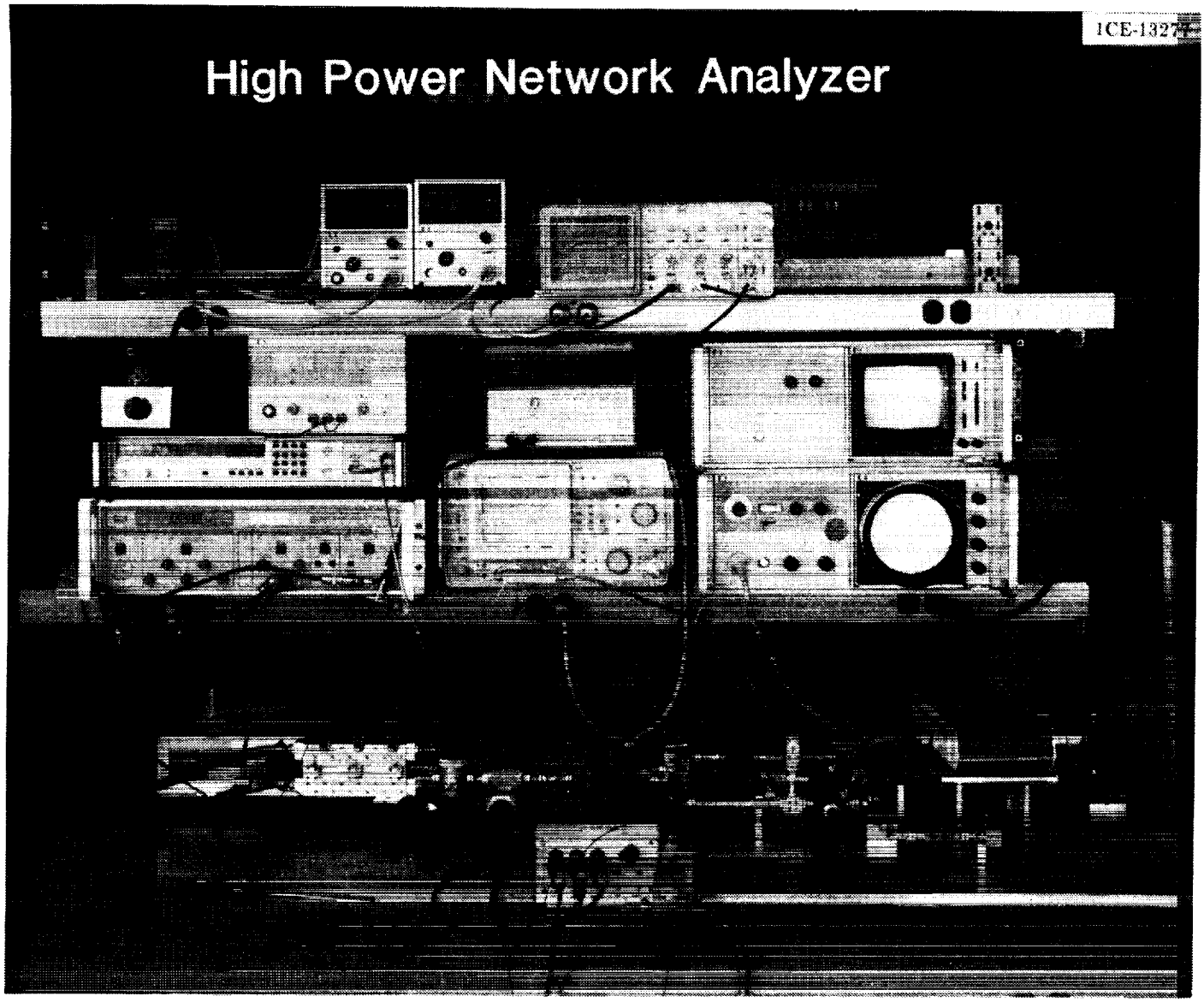

Figure 2-2. Photograph of the High Power 60 GHz Network Analyzer.

equipment. The basic instrument is an HP8410B network analyzer and a custom built waveguide assembly to down-convert the 60 GHz signals to the frequency range of the 8410B. A three-stage IMPATT amplifier was constructed with early prototype circuits to provide nearly 1 W of RF drive across the operating band.

Figure 2-3 is a drawing of the first prototype circuit which was built for this project. The IMPATT diode and a coaxial matching transformer are located at the end of a coaxial transmission line. This coaxial line passes through the broad wall of a reduced-height waveguide, resulting in strong coupling between the waveguide and the coax. One end of the reduced-height waveguide is terminated with a short circuit, while the other end is interfaced to the mating waveguide through a two-section transformer. One section of the transformer is machined into the housing, while the other is in a removable plate. DC power is applied to the exposed end of the bias pin at the top of the drawing. The pin passes through a bias choke, which prevents RF leakage, and then becomes the center conductor of the coaxial line. The tip of the bias pin touches the cap of the IMPATT diode, and a spring (not shown) applies pressure to this contact.

Figure 2-4 is a photograph of this circuit. The housing is made from a single block of aluminum, and the waveguide sections are made by electric discharge machining. All internal parts which were discussed in conjunction with the module drawing are visible in this photograph. The waveguide flange is very smooth and flat in order to make a good RF interface and allow good thermal transfer to the combiner plate.

Figure 2-5 is a polar plot of the reflection coefficient S_{22} of the circuit for three different heights of the removable waveguide transformer. The reference plane is at the end of the coaxial transmission line, labelled "Port 2" in Figure 2-3. When the transformer height is 0.074 inches (full height waveguide), S_{22}

PBN-91-0166

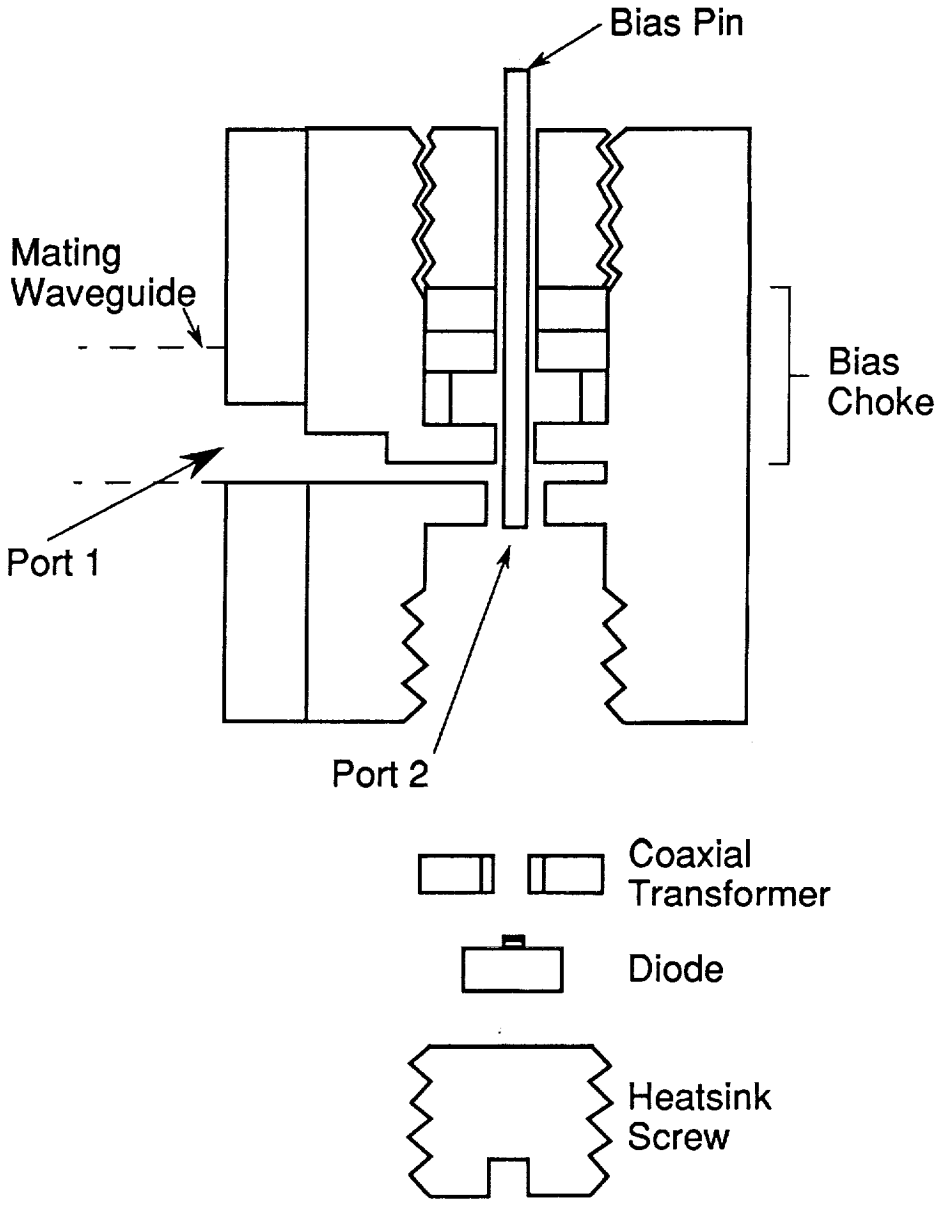

Figure 2-3. Cross Section of the First Prototype 60 GHz IMPATT Amplifier Module.

ORIGINAL PAGE
BLACK AND WHITE PHOTOGRAPH

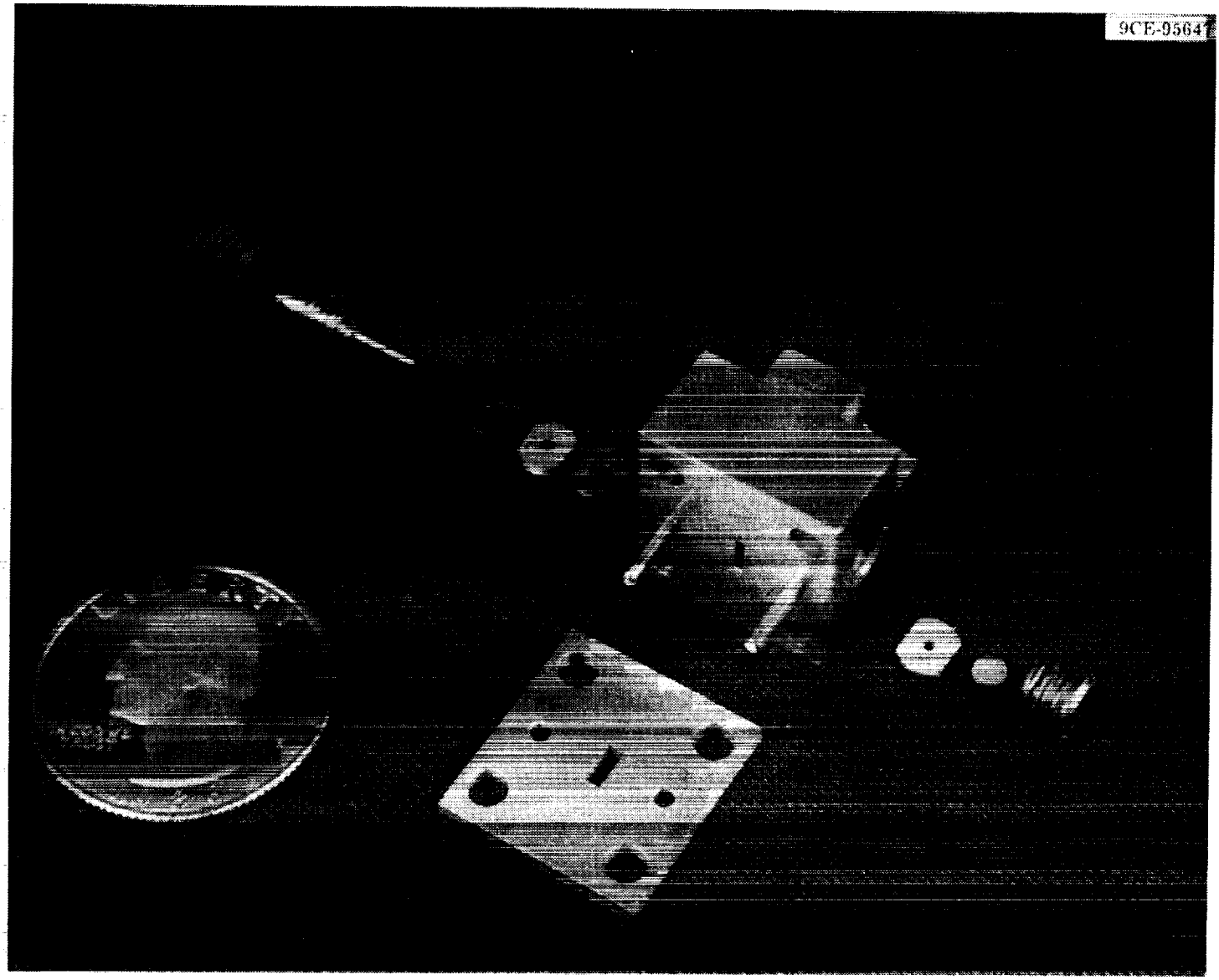

Figure 2-4. Photograph of the First Prototype IMPATT Amplifier Module.

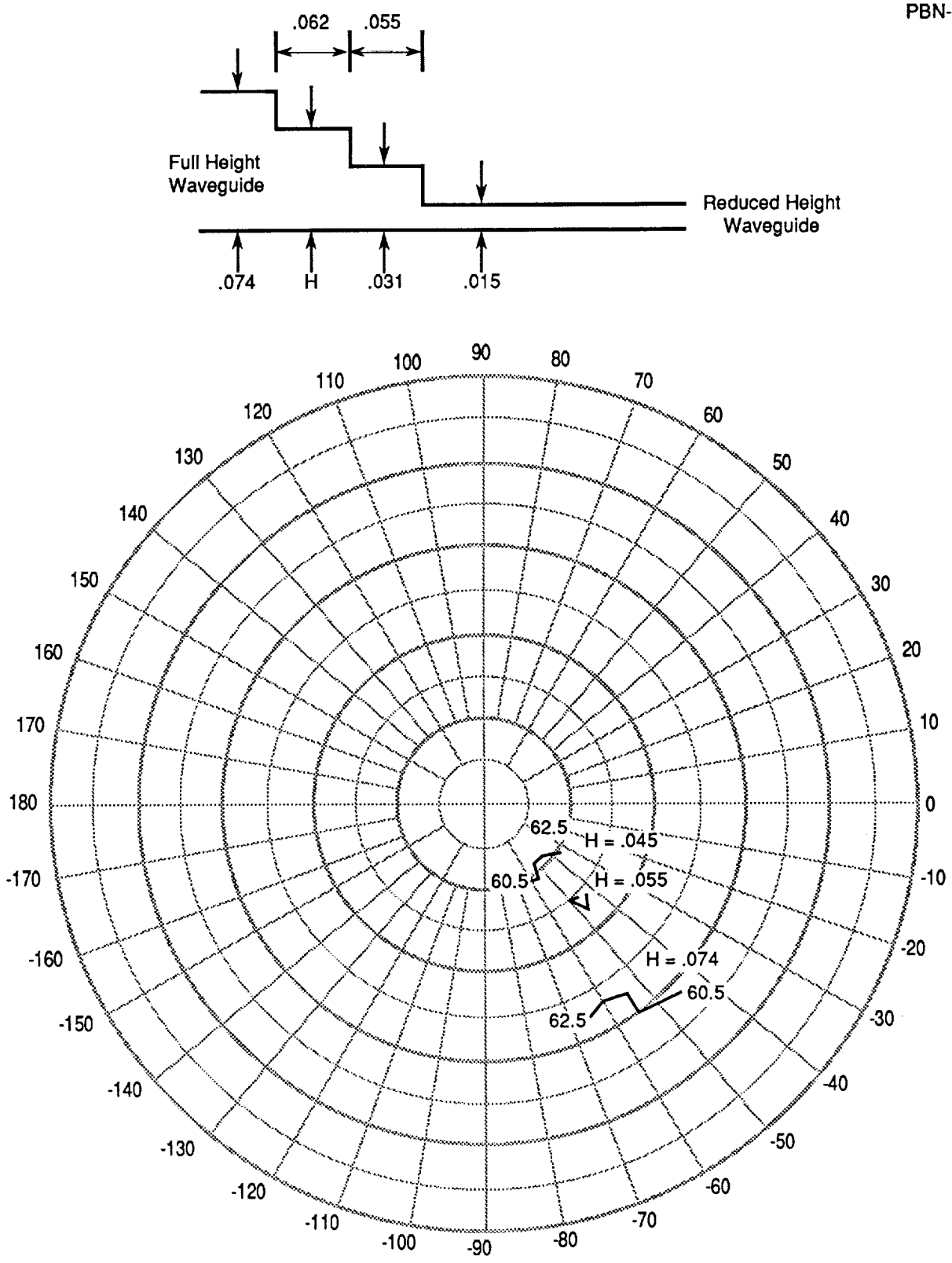

Figure 2-5. Circuit Impedance Measurements of the First Prototype IMPATT Module Using Three Different Waveguide Transformers.

is far from the center of the chart and moving clockwise with increasing frequency. At a height of 0.055 inches, the data is closer to the center of the chart and is insensitive to frequency. The final measurement at a height of 0.045 inches follows the same trend of moving closer to the center of the chart, and the data moves counterclockwise with increasing frequency.

The design goal for the passive circuit was to have S_{22} near the center of the chart and moving counterclockwise to create a double-tuning effect. The result with the 0.045-inch high transformer has about the right arc length, but is not close enough to the center to be optimum.

Figure 2-6 shows a later S_{22} result along with some additional data. The height of the removable transformer was decreased still further to move S_{22} closer to the center of the chart, but the frequency sensitivity increased significantly.

The impedance of the IMPATT diode with its low impedance matching transformer was measured by installing these two components in the previously characterized module. The impedance of the entire module was measured on the high power network analyzer, and the data was referred through the S-parameters of the circuit. The reciprocal of the reflection coefficient of the diode and its low impedance matching transformer ($1/\Gamma_d$) is plotted in Figure 2-6 at two RF drive levels. The data was measured under full bias current conditions and the added power of the diode is noted at each point. This measurement capability is essential for a good understanding of the operation of the circuit.

The distance between S_{22} and $1/\Gamma_d$ should be constant across the operating band to achieve a flat gain response. The diode and its coaxial transformer form a single tuned resonant circuit, and $1/\Gamma_d$ moves counterclockwise with increasing frequency. To keep the distance between S_{22} and $1/\Gamma_d$ constant constant across the band,

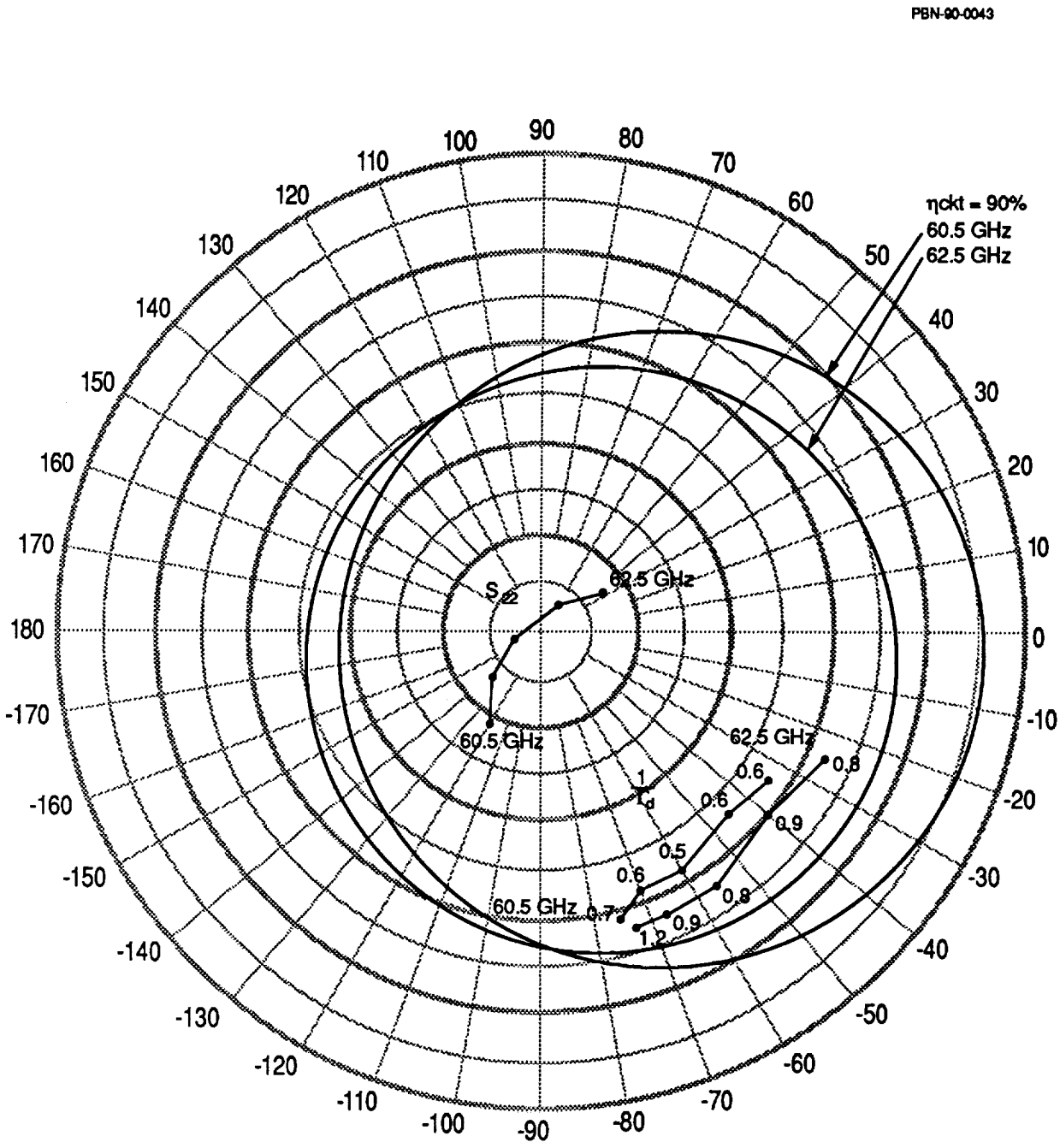

Figure 2-6. Active and Passive Impedance Data from the First Prototype IMPATT Module.

S_{22} must also move counterclockwise with increasing frequency. This requires a double-tuned response from the passive circuit.

In this particular case, the average distance between the two sets of data is about correct for generating the desired circuit gain, but the gain is higher at the edges of the band than at the middle. This is because the S_{22} arc is too long, and the ends hook too far toward the $1/\Gamma_d$ data.

Two circles are also drawn in Figure 2-6 which are circuit efficiency contours. Circuit efficiency is defined as the ratio of the added power of the amplifier circuit at the output flange divided by the added power of the diode.

$$\eta_{ckt} = \frac{\text{added power of circuit}}{\text{added power of diode}}$$

For a given circuit and frequency, the circuit efficiency is a function of the 2-port S-parameters of the circuit and the $1/\Gamma_d$ of the diode and its transformer. In principle, $1/\Gamma_d$ can be anywhere on the chart depending on the characteristics of the diode and transformer. The efficiency of the circuit can be calculated for any hypothetical value of $1/\Gamma_d$, and the set of points which have the same circuit efficiency form a circle.

Figure 2-6 shows the 90 percent circles at the band edges. The circuit efficiency is lower on the outside of the circles, and approaches 95 percent at the centers of the circles. Our amplifier design requires the IMPATT circuits to have a minimum circuit efficiency of 90 percent, so $1/\Gamma_d$ must be tuned to lie within the 90 percent efficiency circles.

A complete circuit design requires many factors to be weighed simultaneously. Achieving the correct gain means that S_{22} and $1/\Gamma_d$ must be the right distance apart. Minimizing ripple across the

operating band requires this distance to be held very constant across the operating band. Maximum efficiency is obtained when $1/\Gamma_d$ is near the center of the 90 percent efficiency contours. The complete set of data shown in Figure 2-6 illustrates a reasonably good balance of all these requirements.

There were two improvements which we wanted to make to the electrical design of the circuit. Decreasing the length of the S_{22} arc would improve the gain flatness. Also, the S_{22} arc is tilted toward the fourth quadrant of the polar chart by about 40°. If S_{22} could be rotated so that it faced directly to the right, $1/\Gamma_d$ could be rotated up to a higher value of circuit efficiency while remaining parallel to the S_{22} arc.

These improvements were impossible to make with the original circuit design. A second prototype circuit, shown in Figures 2-7 and 2-8, was found to be superior. The removable waveguide transformer was eliminated, and the height and length of the fixed waveguide transformer were chosen to make a small S_{22} arc in the fourth quadrant, shown in Figure 2-9. A high impedance coaxial spacer was then added to rotate the S_{22} approximately 130° clockwise to the horizontal axis. The distance from the center of the chart can be varied by changing the impedance of this spacer as illustrated in Figure 2-10.

These electrical changes corrected the shortcomings of the first prototype. Figures 2-11 and 2-12 illustrate the performance of the second prototype in two ways. Figure 2-11 is a polar plot which shows that S_{22} is positioned near the center of the chart and its arc length is quite short. $1/\Gamma_d$ is shown at drive levels of 0.4, 0.6 and 0.8 watts, and the coaxial transformer has been designed to put this data closer to the horizontal axis. The data in Figure 2-12 was measured on the same circuit, and illustrates the flat frequency response and smooth saturation of the circuit.

PBN-90-265

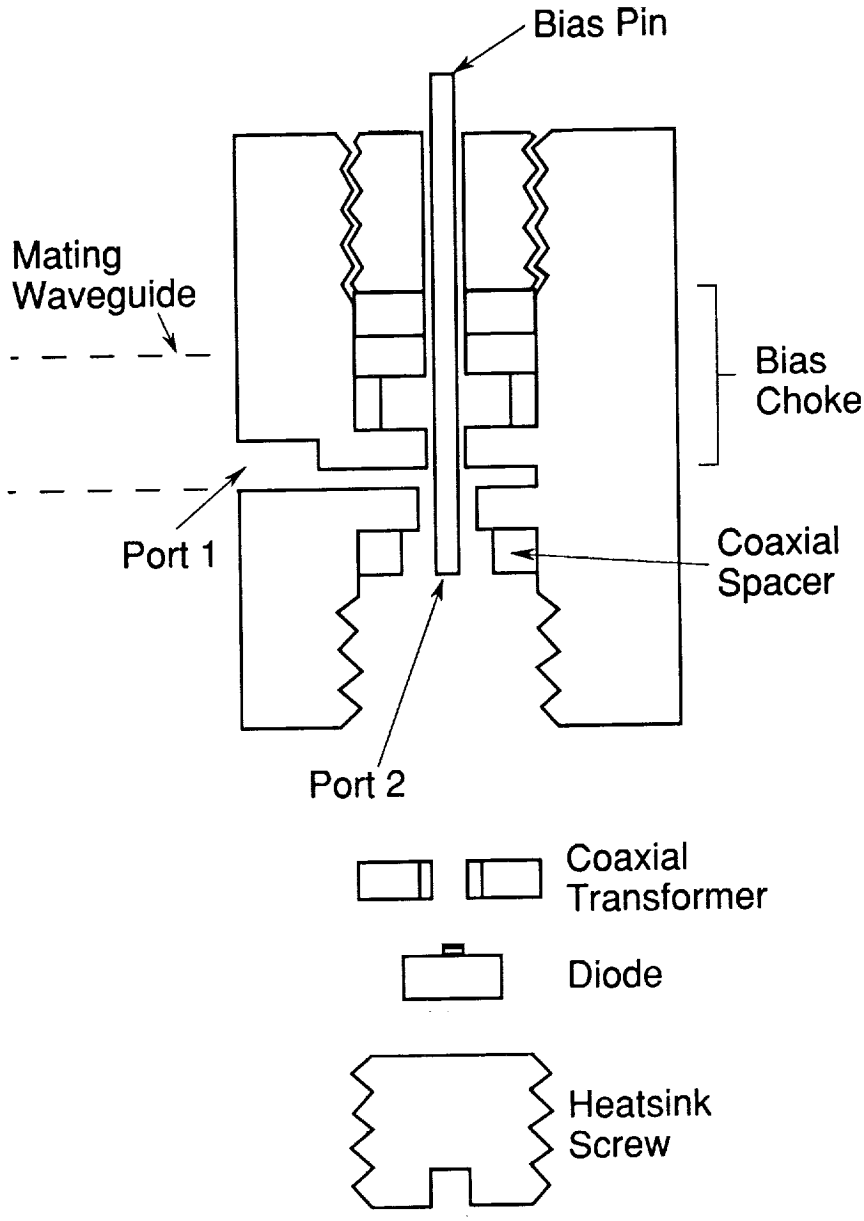

Figure 2-7. Cross Section of the Second Prototype IMPATT Amplifier Module.

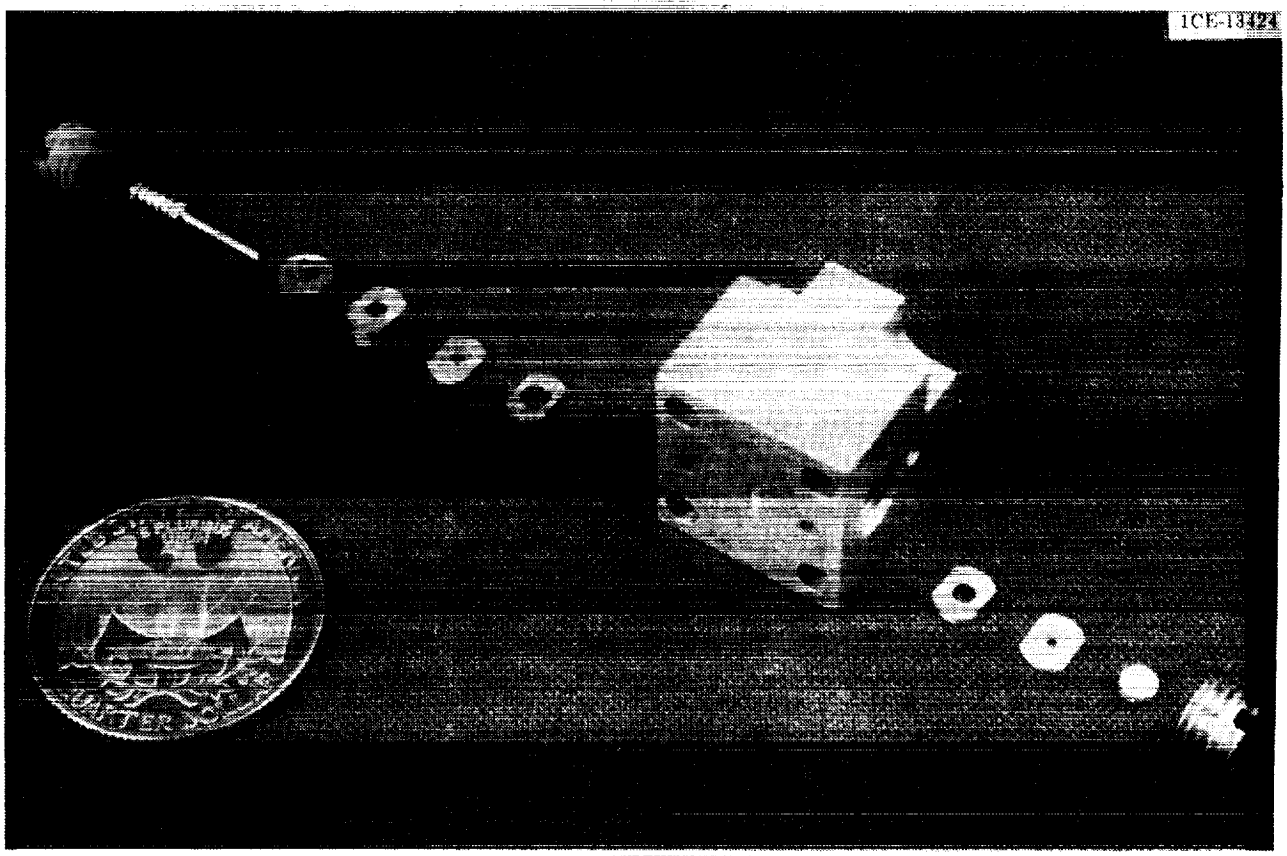

Figure 2-8. Photograph of the Second Prototype IMPATT Amplifier Module.

PBN-90-262

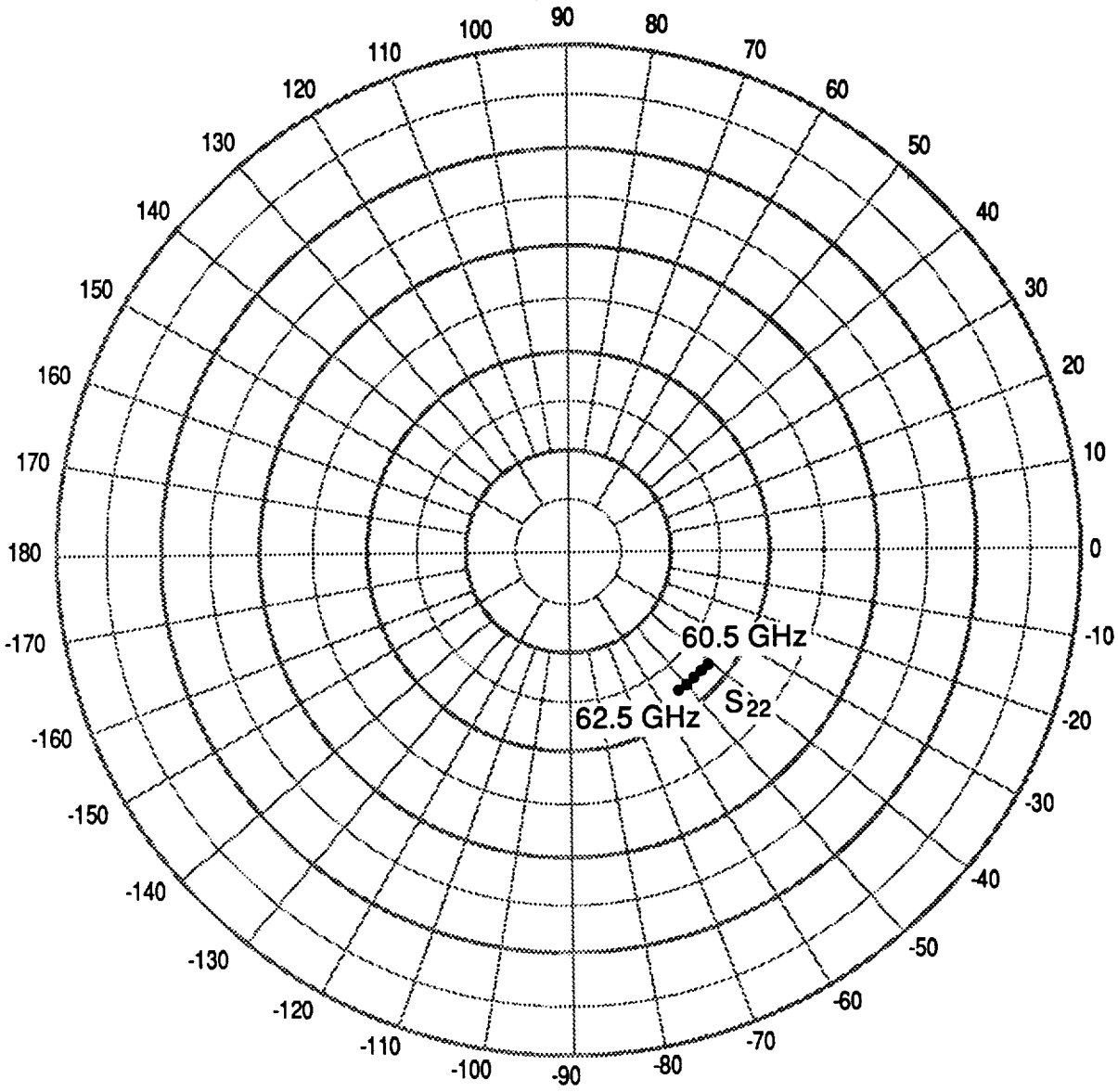

Figure 2-9. Circuit Impedance of the Second Prototype IMPATT Module with the Coaxial Spacer Removal.

PBN-90-261

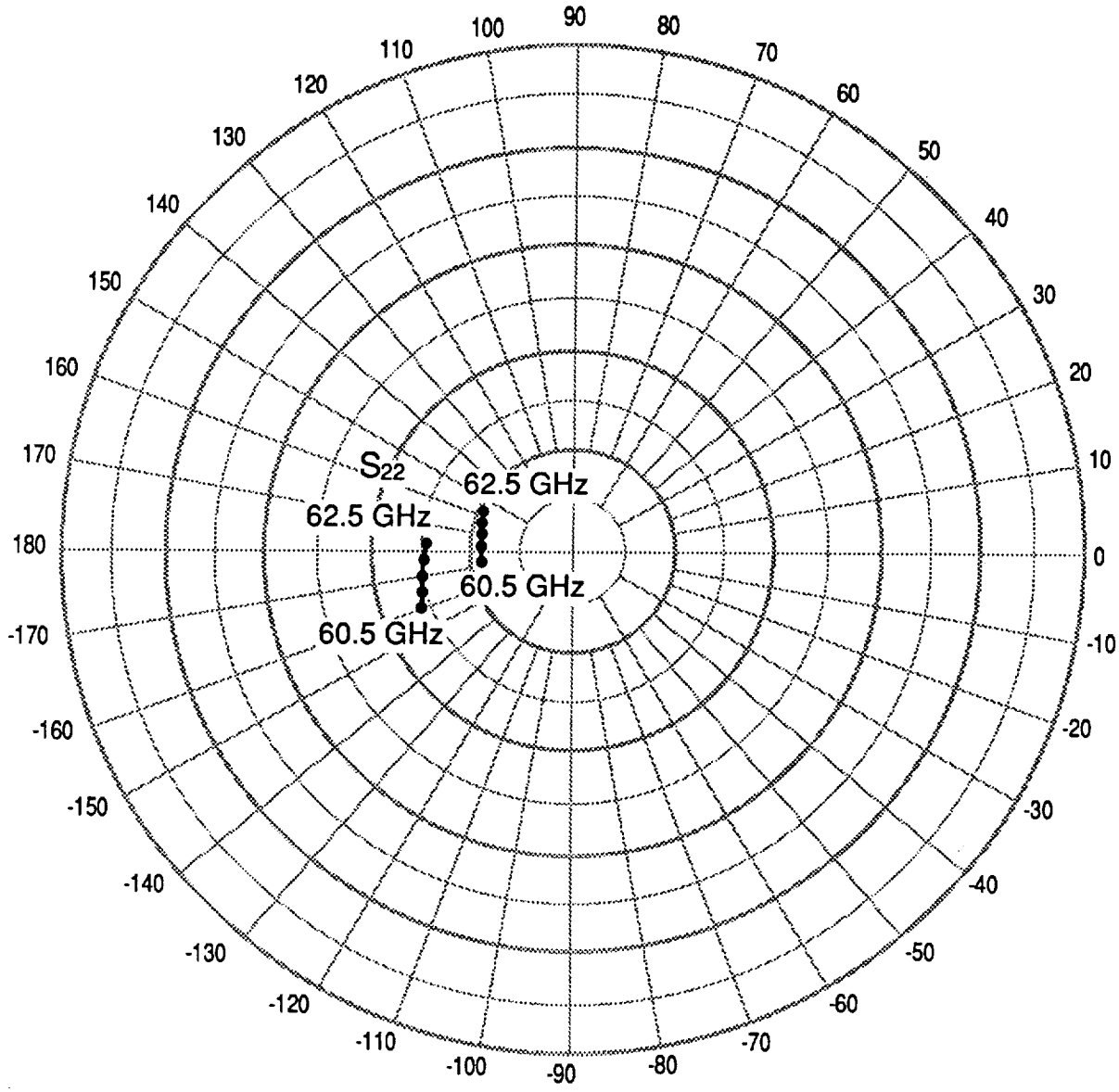

Figure 2-10. Circuit Impedance of the Second Prototype IMPATT Module with Two Different Coaxial Spacers.

PBN-90-716

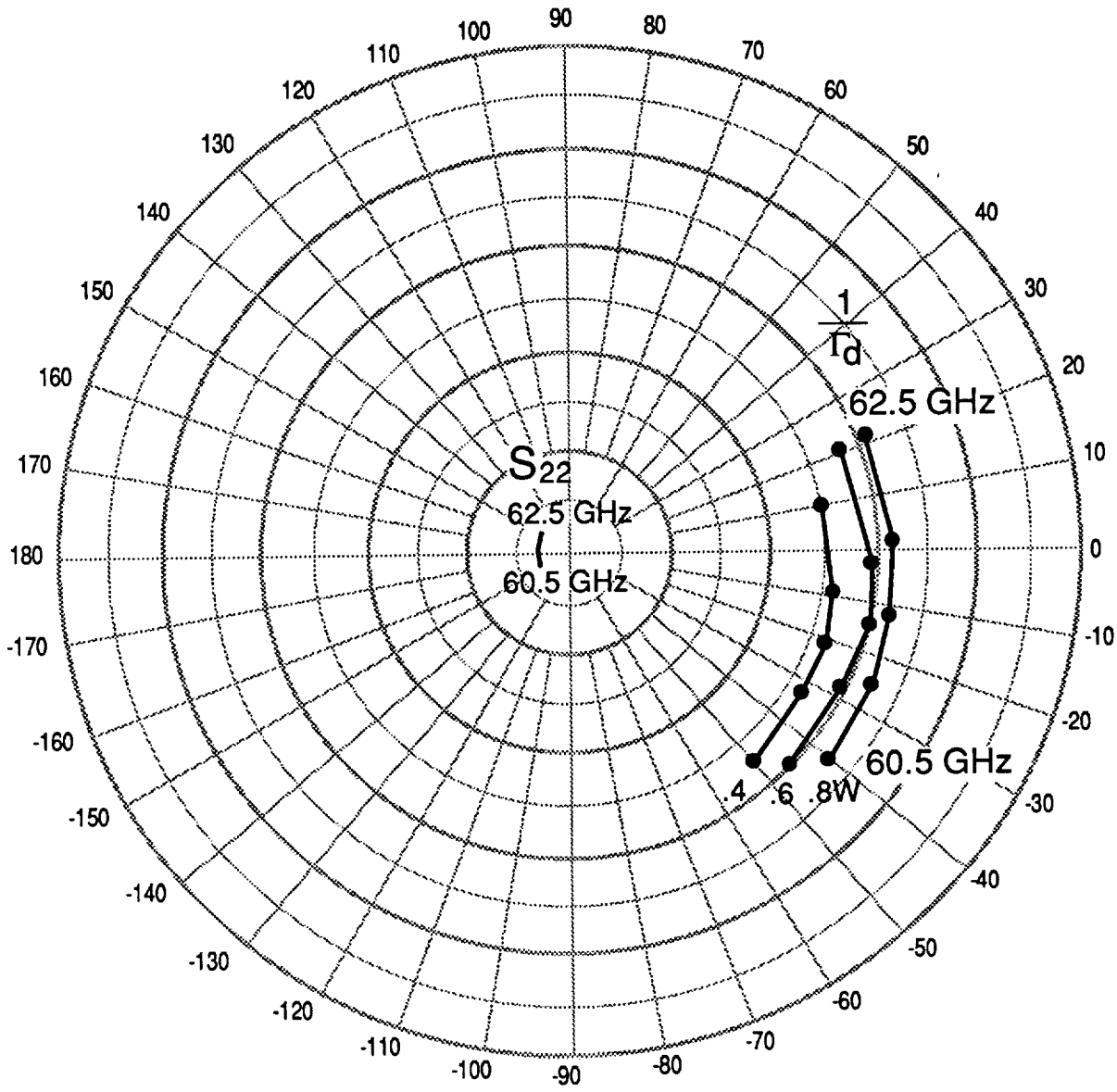

Figure 2-11. Polar Plot of the Device and Circuit Impedances of the Second Prototype IMPATT Module.

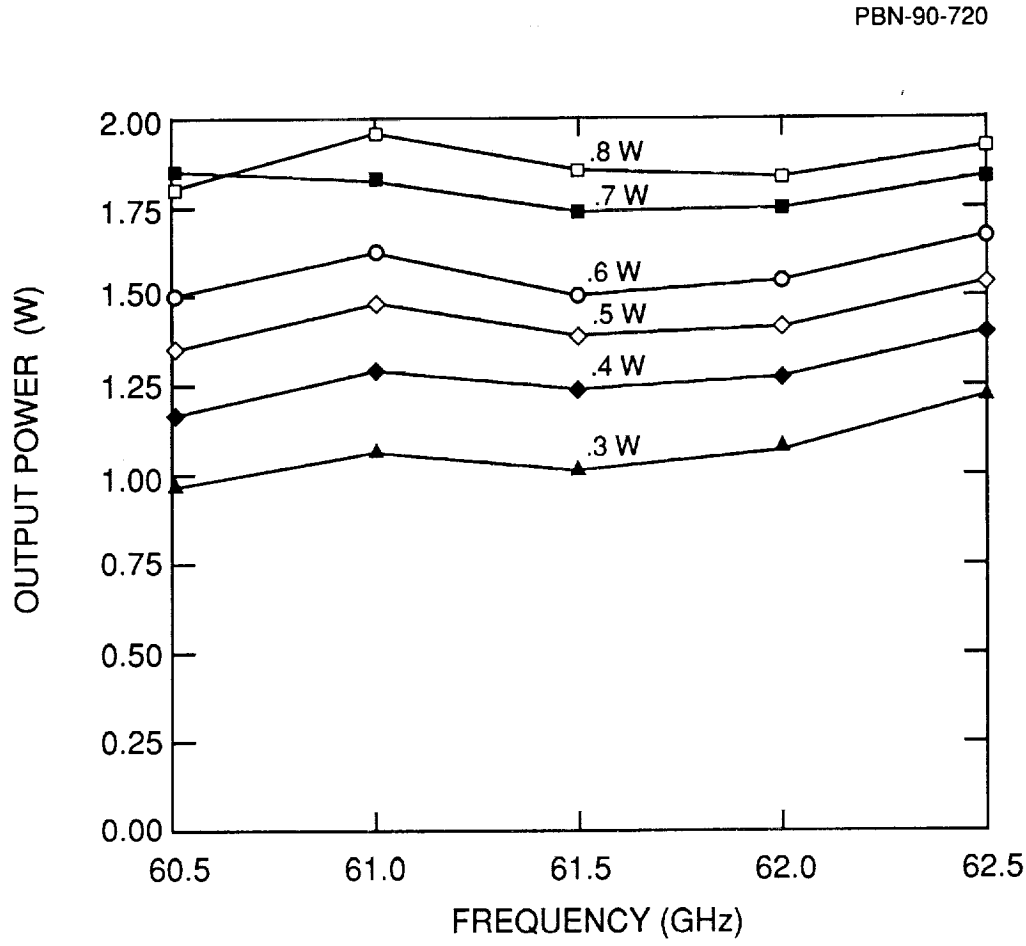

Figure 2-12. Output Power of the Second Prototype IMPATT Module.

The final design of the IMPATT module which was used to construct the amplifier is electrically identical to the second prototype. The mechanical design of the housing was changed slightly to accommodate the bias regulator circuit board as shown in Figure 2-13.

The same housing design was used to build the high gain circuits for the first two stages, but some of the internal parts are different. A smaller area diode was used and the bias current was reduced because these stages add very little RF power. A lower impedance transformer was also employed to increase the gain of the circuit.

2.3 Combiner Plate

The combiner plate is a Raytheon invention which was used in this contract. The details of this component are proprietary, but the general function will be described below.

A combiner plate contains a series of waveguide junctions and interconnecting waveguide runs which sum the output powers of a number of reflection amplifiers. The NASA amplifier has seven stages, and the waveguide networks for all the stages were built into the same combiner plate.

The waveguide combiners were designed for extremely low loss, good port match and high isolation. The transmission loss through the 8-way combiner is about 0.35 dB per pass, as shown in Figure 2-14, and the smaller stages have even lower loss. This data was taken by shorting the module ports and measuring the two-pass attenuation on the automatic network analyzer. The one-pass attenuation is obtained by dividing this result in half. The input port match, shown in Figure 2-15, was generally better than -25 dB, and was -22 dB in the worst case. Module port isolation was approximately -25 dB.

ORIGINAL PAGE
BLACK AND WHITE PHOTOGRAPH

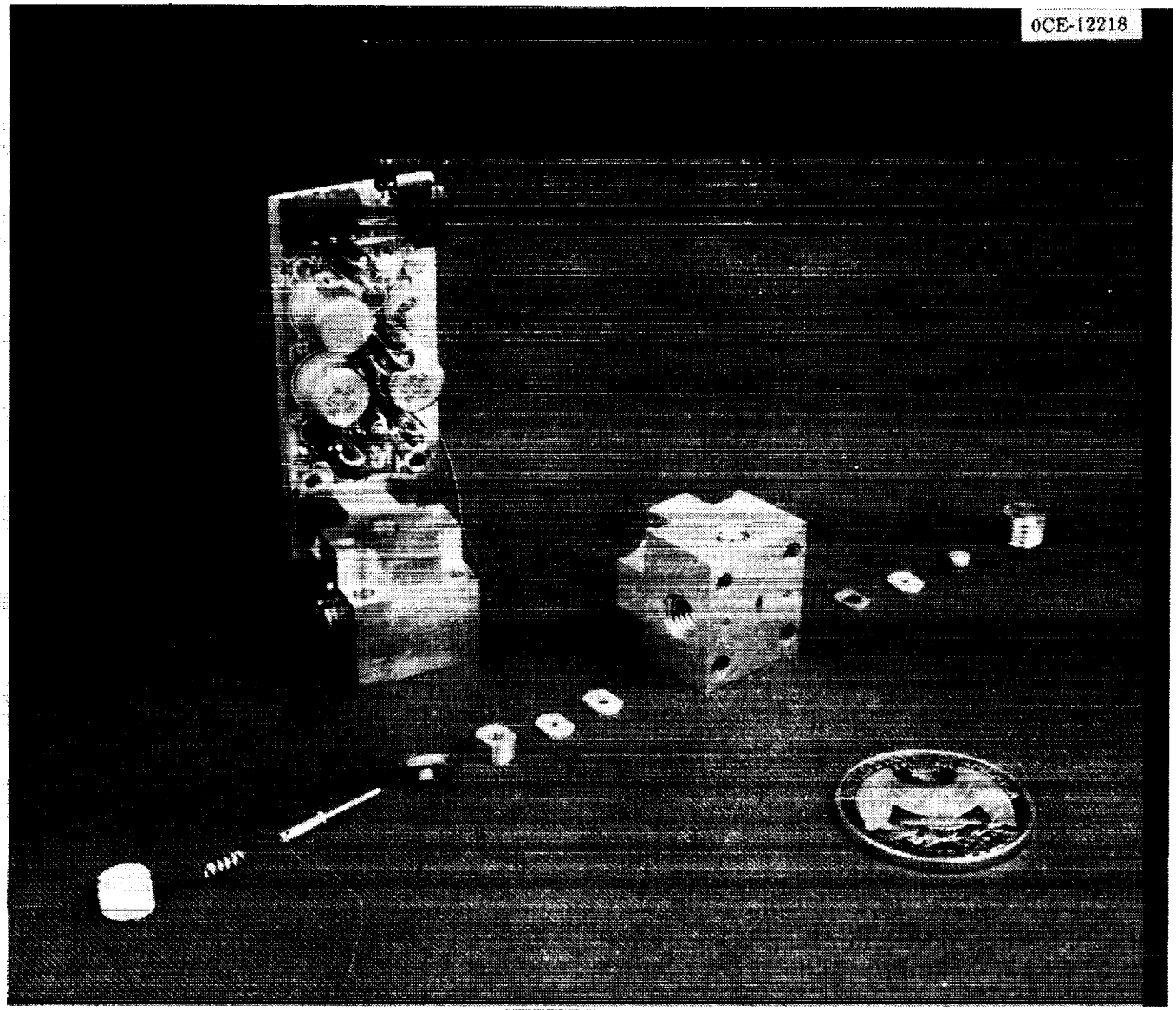

Figure 2-13. Photograph of Assembled and Disassembled IMPATT Modules used to Construct the Amplifier.

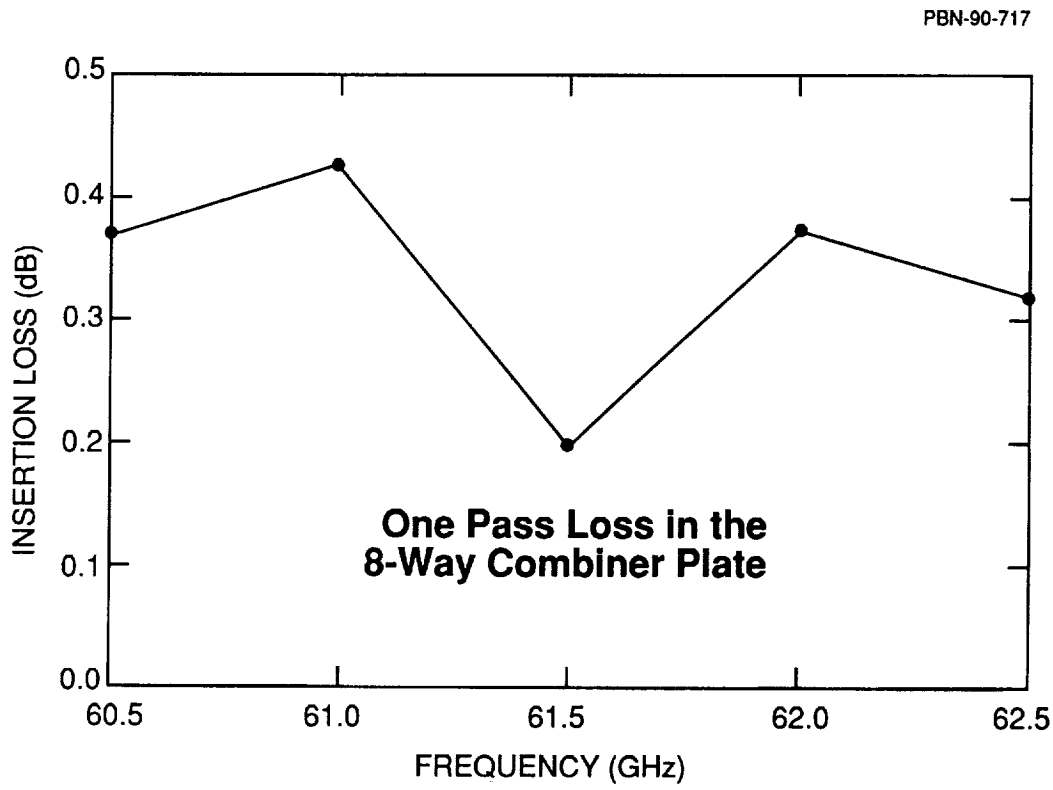

Figure 2-14. Insertion Loss of the 8-Way Combiner Network in the Combiner Plate.

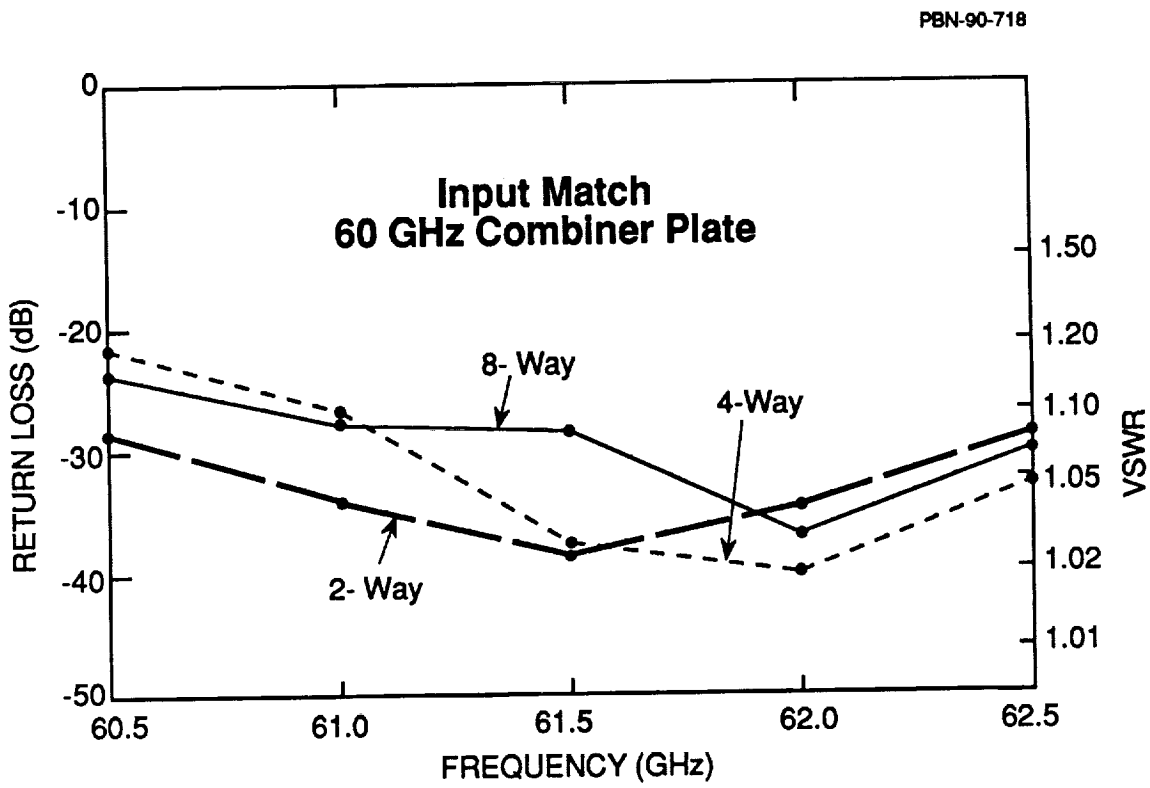

Figure 2-15. Input Match of the Three Combiner Networks in the Combiner Plate.

These excellent electrical properties were fundamental to the success of the amplifier. Low combiner loss conserves the RF power generated by the IMPATT diodes, resulting in high output power and efficiency. Good port match allows the RF components to be screwed together at the final assembly and generate their optimum performance without a complicated, interactive tuning procedure. Module port isolation allows the amplifier to degrade gracefully in case of an IMPATT diode or bias regulator failure.

The combiner plate is fabricated from aluminum, because light weight is very important for a spacecraft component. Copper has better electrical conductivity, but it is three times heavier than aluminum. We tried an experiment to see if the attenuation in the combiner plate could be reduced by plating copper over the aluminum surface. This would combine the electrical advantage of copper with the weight advantage of aluminum.

A 10-inch straight section of aluminum waveguide was fabricated using the same machining techniques that were used in the combiner plate. The transmitted power was measured across the operating band with a chromated aluminum surface and with the copper plated surface. Figure 2-16 shows that the plating reduced the attenuation by about 20 percent, which is what would be predicted from the difference in electrical conductivities of the two metals.

A 20 percent reduction in the already low attenuation of the combiner plate would not have a major impact on the overall amplifier efficiency. However, the plating process is very inexpensive and the benefit would be worth the added cost. We plated the combiner plate and found that the attenuation was lower at some frequencies but higher at others. A two-pass return loss measurement is not as accurate as the simple transmission measurement that could be used for the waveguide test piece. We

PBN-90-1320

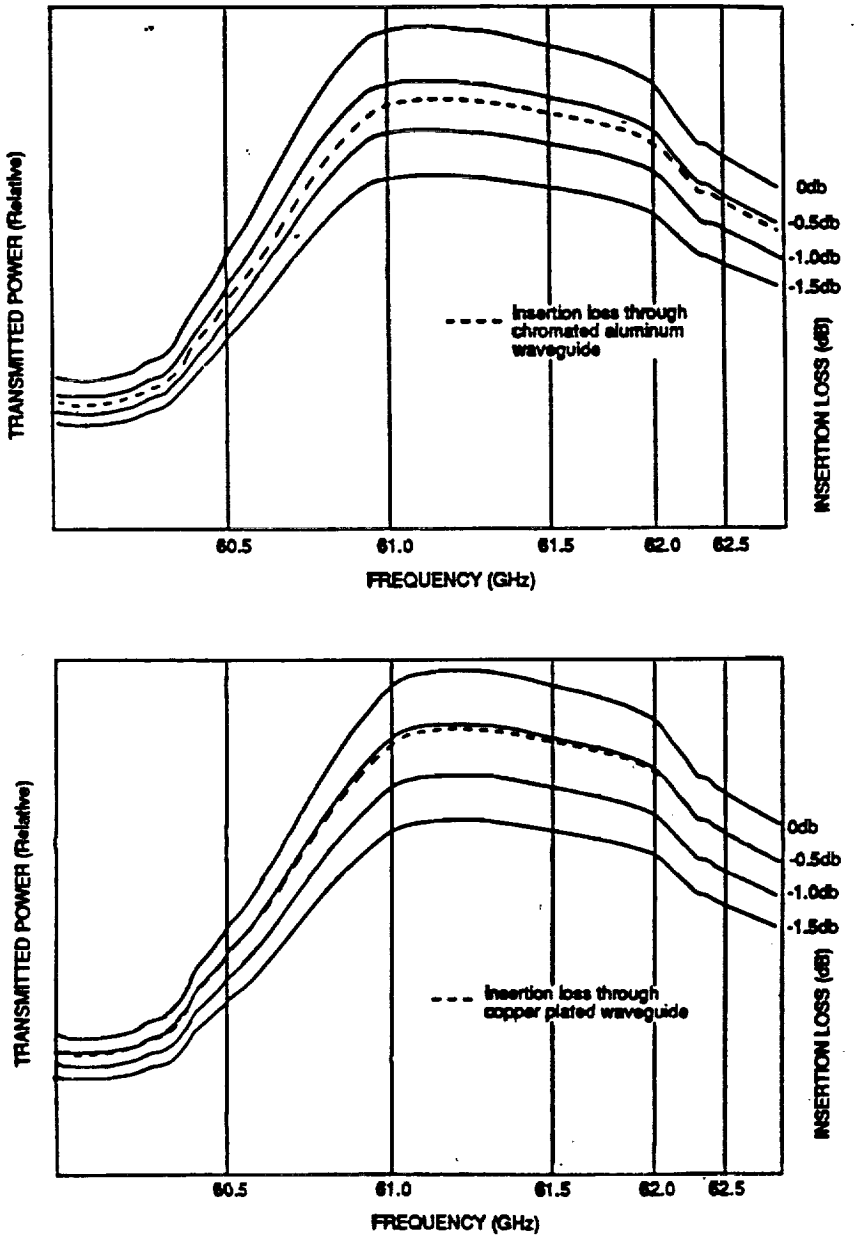

Figure 2-16. Transmission Loss of an Aluminum Waveguide (upper graph). Transmission loss of the same waveguide with copper plating (lower graph).

concluded that the attenuation was probably better with the copper plating, but we could not measure the difference.

The RF measurements were somewhat ambiguous, but a definite disadvantage to the copper plating was also found. A chromate conversion coating was applied over the plating but the copper surface still oxidized badly. This was particularly true on the outside surfaces where the plate was handled. In addition, galvanic corrosion may occur over a long period of time between the copper plating and the aluminum IMPATT modules. We could not think of another coating which would be a better barrier without spoiling the electrical conductivity of the copper surface.

In the end, we decided to remove the plating from the combiner plate and use it with the original chromated aluminum surface. The idea to plate a high conductivity metal over a light-weight, lower conductivity metal has merit. Perhaps a better process can be developed in the future.

2.4 Isolator/Circulator Assemblies

There are only a few companies which manufacture V-band circulators, and we chose Electromagnetic Sciences because their products have the best electrical performance. Originally, they offered 1-junction circulators but not 2-junction isolator/ circulator assemblies. This new component was developed, and Figure 2-17 is a photograph of the 1-junction and 2-junction designs. The specifications for these devices are listed below.

ORIGINAL PAGE
BLACK AND WHITE PHOTOGRAPH

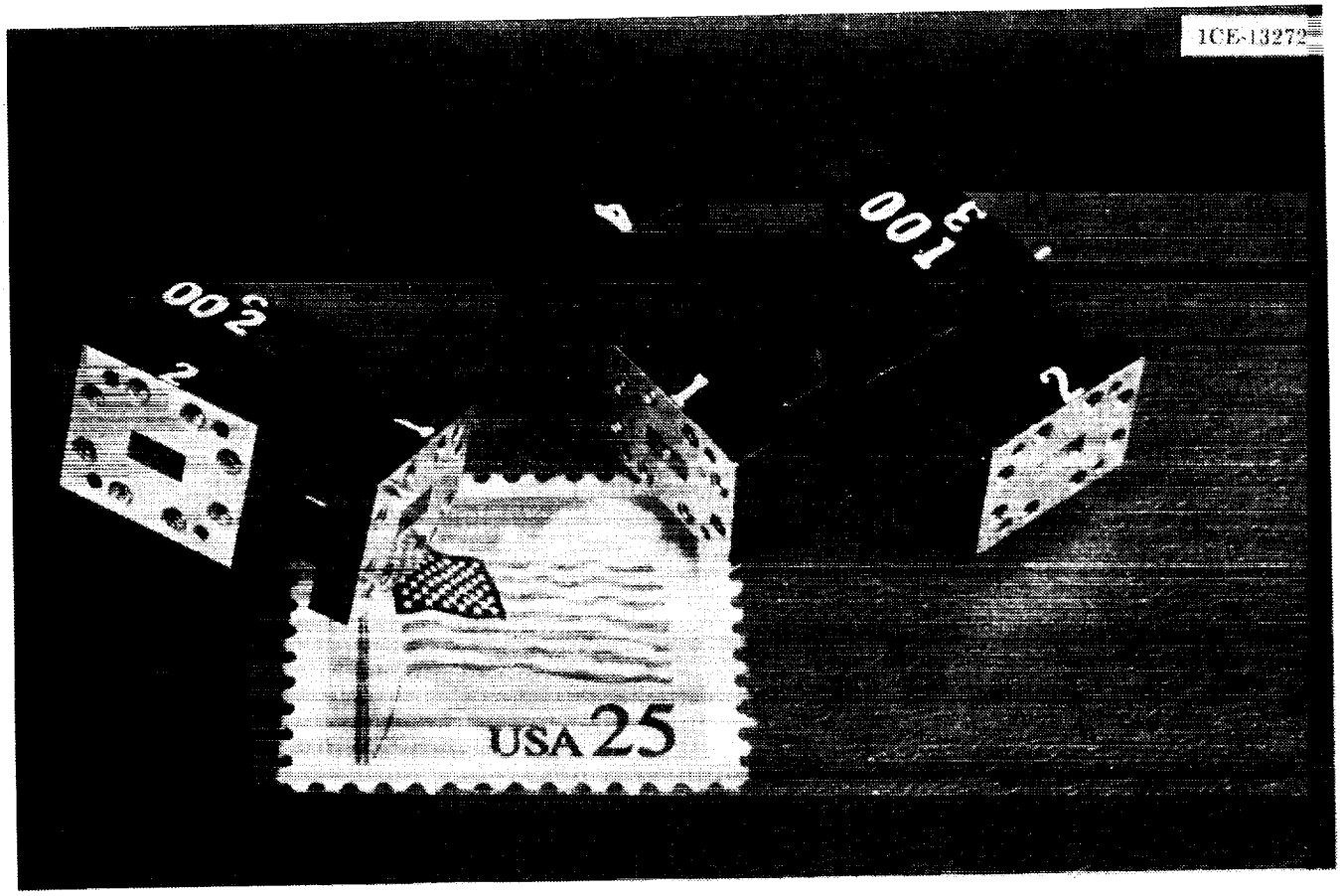

Figure 2-17. Photograph of a 1-Junction Circulator and a 2-Junction Circulator.

Circulator and Isolator Specifications

Frequency	61.5 GHz
Bandwidth	2 GHz
Insertion Loss	0.3 dB/pass maximum
	0.2 dB/pass typical
Isolation	15 dB minimum
	20 dB typical
VSWR	1.2 maximum
RF Power	10 watts into isolator load

2.5 Electronic Circuits

Two different circuits are used in the amplifier: the bias regulators and a control circuit. Each IMPATT module has a bias regulator circuit attached to it, shown in Figure 2-13, which supplies dc power to the IMPATT diode. The 18 bias regulators are connected to the control circuit through a wiring harness. The control circuit adjusts the bias regulator current according to the baseplate temperature. It also turns the bias regulators off if the RF input signal is absent, preventing a possible oscillation in the IMPATT circuits.

Figure 2-18 is a simplified schematic of the bias regulator circuit, and a photograph is shown as Figure 2-19. When the regulator is turned on, a 10 volt signal is applied to the on/off control input, saturating an enhancement mode FET Q2. A dc voltage of approximately 9 volts is applied to the control input, generating a current through transistor Q1. The current from Q1 is amplified by a current mirror and is applied to the IMPATT diode. The current through Q1 can be changed by varying the control input voltage, which then changes the IMPATT current. The bias regulator can be switched off by dropping the on/off control voltage to zero. The bias regulator can also sense if the IMPATT diode has failed,

PBN-90-2445

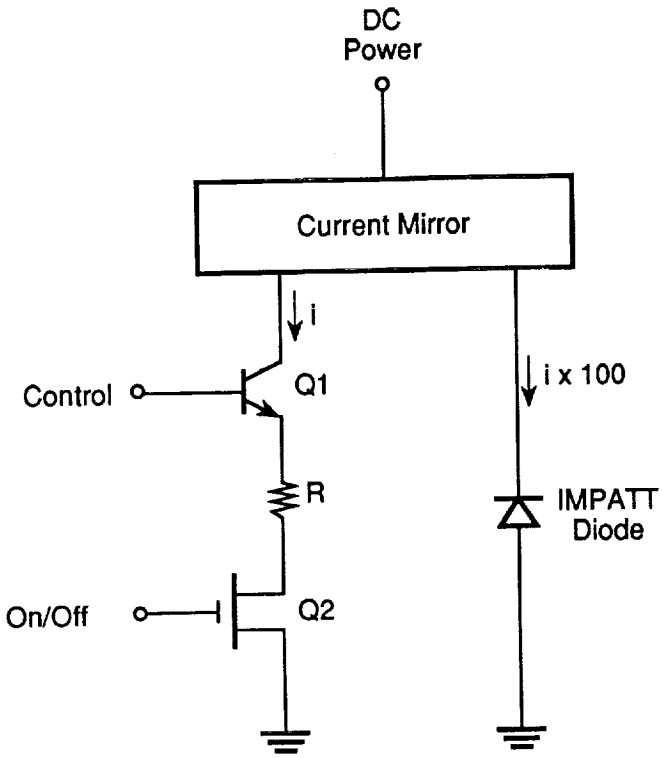

Figure 2-18. Simplified Schematic of the Bias Regulator Circuit.

ORIGINAL PAGE
BLACK AND WHITE PHOTOGRAPH

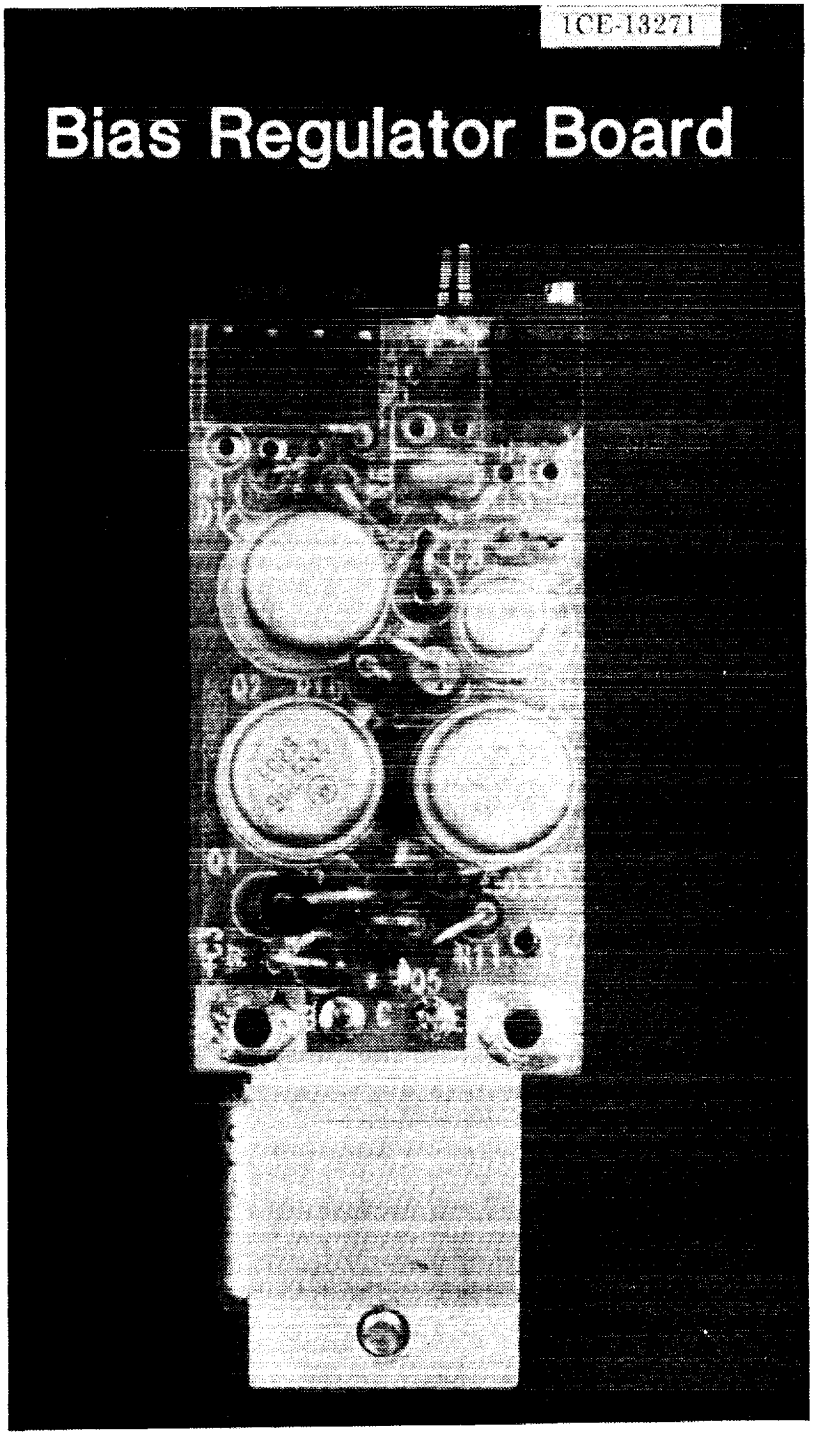

Figure 2-19. Photograph of a Bias Regulator Circuit Board.

and turns off the bias current to prevent overheating in the circuit.

This electronic circuit is particularly good for this application because it regulates the IMPATT bias current without requiring a high power supply voltage. All the IMPATT current flows through the current mirror from the power supply; therefore, the power dissipated in the regulator is proportional to the voltage difference between the IMPATT diode and the power supply. Dissipation must be minimized since the most important goal of this contract is to achieve high overall efficiency. Figure 2-20 shows the output current of the regulator as a function of this voltage difference at several control voltage values. Notice that the flat, constant current region begins with less than a 2 volt drop in each case.

Figure 2-21 is the block diagram of the control circuit for the amplifier, and a photograph is shown as Figure 2-22. The control voltages for the bias regulators are generated by two voltage regulators with temperature compensation. All the high power modules are controlled by one signal, and the two high gain stages are controlled by the other one.

The other function of the control circuit is to turn the bias regulators on and off in response to the RF input power. Most of the IMPATT modules are stable, but this is difficult to guarantee without compromising output power or gain. Figure 1-1 illustrates how we placed a directional coupler and a crystal detector at the amplifier input to sense the RF input signal. If the input signal is present, a current is generated in the crystal and the comparator changes state. The output of the comparator is boosted by a driver, and the resulting signal is used to turn on all 18 bias regulator circuits. This feature also saves power when the amplifier is not operating, an important consideration in space.

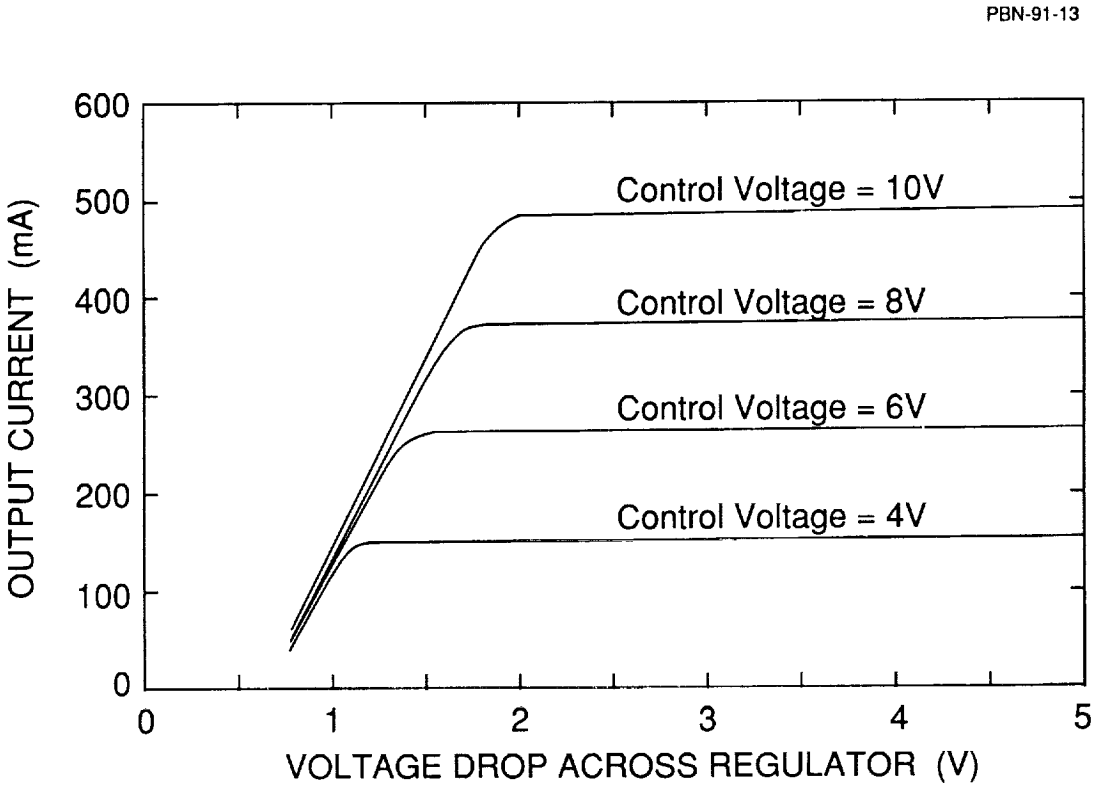

Figure 2-20. Performance of the Bias Regulator Circuit.

PBN-90-2446

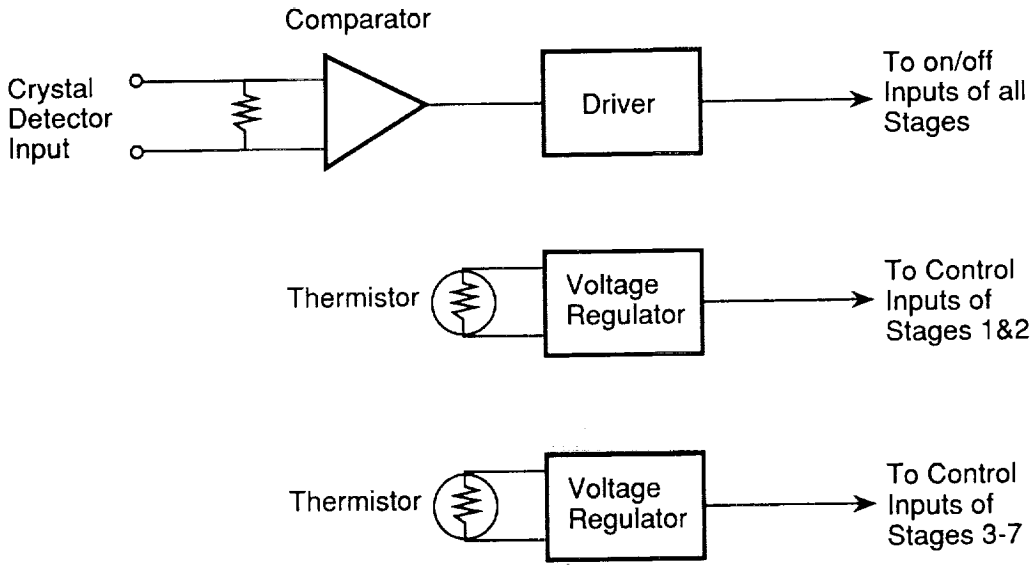

Figure 2-21. Block Diagram of the Control Circuit.

ORIGINAL PAGE
BLACK AND WHITE PHOTOGRAPH

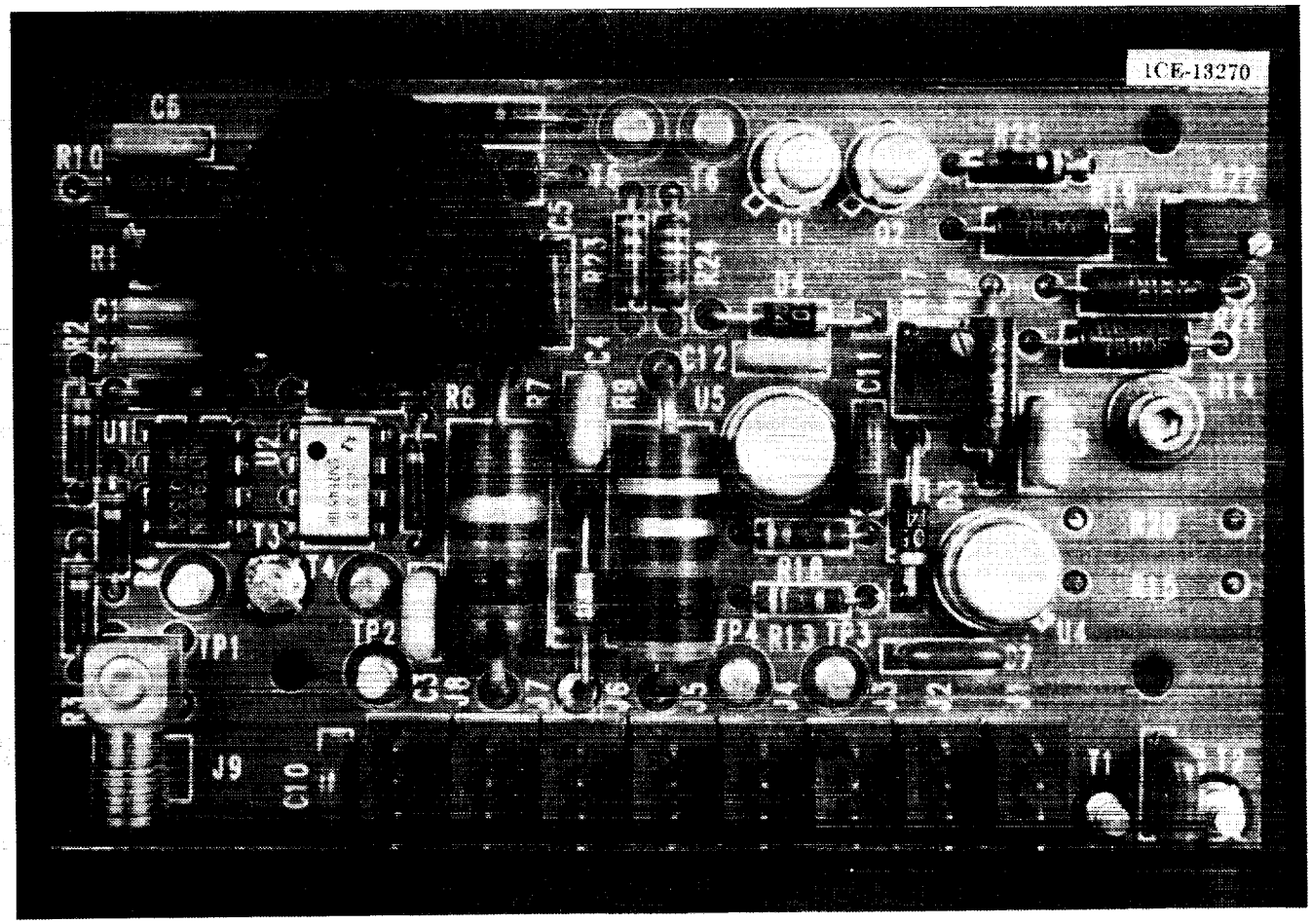

Figure 2-22. Photograph of the Control Board.

The response time of the control circuit and the bias regulators was made as fast as possible. We were able to achieve an overall turn-on time of under 50 nS, and a turn-off time of about 400 nS.

The introduction mentioned that the bias regulators could be built as hybrid circuits to reduce the size of the amplifier. This approach is being used successfully with other solid-state amplifiers at Raytheon, but would have been too expensive for this development contract. Hybridizing the bias regulators will be a low risk engineering task that can be done at a later time when a space qualified amplifier is developed.

2.6 Thermal Design

A amplifier which is built on a combiner plate can be cooled easily in space. The heat which is generated in the IMPATT modules is conducted to the combiner plate where it can be removed through the flat bottom surface. We designed an air-cooled heat exchanger for this prototype amplifier so that it could be operated conveniently in the laboratory. Figure 2-23 is a photograph of the chassis from the front, showing the cooling fins and the flat cold plate where the combiner plate is attached. Figure 2-24 is a photograph from the rear, showing the small "muffin" fan and its plenum. This heat exchanger is able to keep the temperature of the amplifier components at less than 10°C above the ambient air temperature.

ORIGINAL PAGE
BLACK AND WHITE PHOTOGRAPH

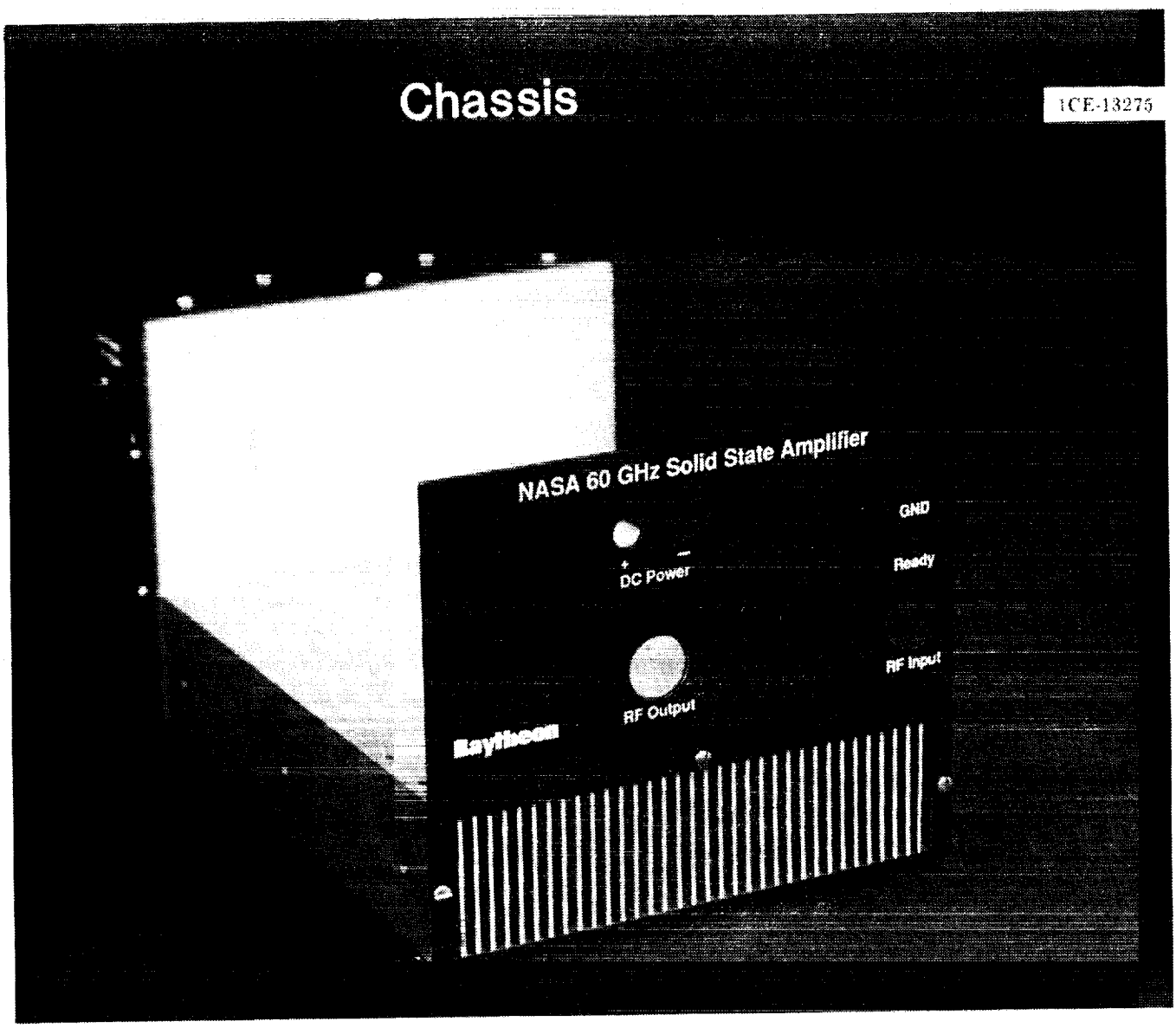

Figure 2-23. Front View of the Amplifier Chassis.

ORIGINAL PAGE
BLACK AND WHITE PHOTOGRAPH

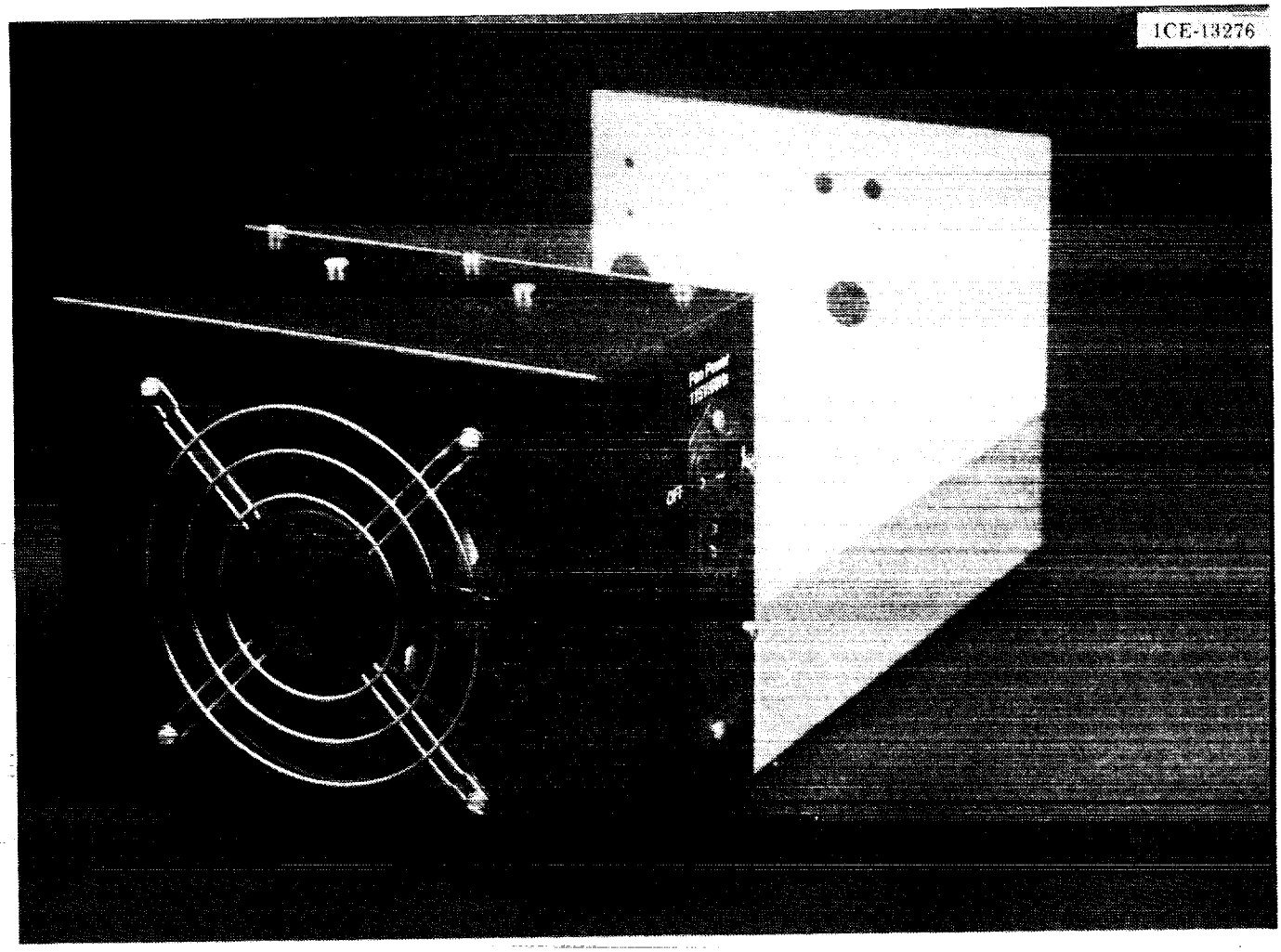

Figure 2-24. Rear View of the Amplifier Chassis.

3.0 AMPLIFIER ASSEMBLY AND TEST RESULTS

The previous section described all the major RF and electrical components which were used in the amplifier. This section will describe the assembly process and the test results.

3.1 Amplifier Assembly and Output Power Measurements

Our design philosophy was to design the amplifier components so that they would not interfere with each other. Then if each component was producing its optimum performance, the performance of the entire assembly would automatically be optimized as well. Not only is this approach easier to implement than one where the components "load pull" each other, this philosophy also achieves the best results.

Chronologically, stages 4 through 7 were assembled first. The high power, low gain modules in these stages have the same electrical requirements, and these stages compose the bulk of the total effort. Therefore, we were very interested in assembling these stages to discover if there were any problems. As it turned out, the performance closely followed the spreadsheet analysis of the amplifier design, shown in Table 3-1. Once the high power portion of the amplifier was assembled and tested, the high gain stages were added.

Figure 3-1 is a very interesting set of data which can be compared to the spreadsheet analysis in Table 3-1. The graph shows the output power of each amplifier stage at the circulator output. This corresponds to line 10 across the spreadsheet. While the results are slightly below the design values in some cases, the overall functioning of the amplifier was predicted very closely by the analysis.

TABLE 3-1

Spreadsheet Analysis of the 7-Stage Amplifier Design

		Stage 1	Stage 2	Stage 3	Stage 4	Stage 5	Stage 6	Stage 7
1.	Diodes in stage	1	1	1	1	2	4	8
2.	P_{in} to stage	1.0 mW	9.9 mW	91 mW	0.67	1.34	2.64	5.22
3.	Input losses (dB)	1.65	0.65	0.65	0.65	0.70	0.50	0.60
4.	P_{in} to module (W)	0.70 mW	8.5 mW	79 mW	0.58	0.58	0.58	0.58
5.	Module gain (dB)	12.0	11.0	9.8	4.1	4.1	4.1	4.1
6.	P_{added} of module (W)	10 mW	99 mW	0.67	0.92	0.92	0.92	0.92
7.	P_{added} of diode (W)	11 mW	110 mW	0.74	1.02	1.02	1.02	1.02
8.	P_{out} of module (W)	11.1 mW	107 mW	0.75	1.50	1.50	1.50	1.50
9.	Output losses (dB)	0.50	0.70	0.50	0.50	0.55	0.60	0.70
10.	P_{out} of stage (W)	9.9 mW	91 mW	0.67	1.34	2.64	5.22	10.21
11.	Stage gain (dB)	10.0	9.6	8.7	3.0	2.9	3.0	2.9
12.	P_{added} of stage (W)	8.9 mW	81 mW	0.58	0.67	1.30	2.58	4.99
13.	Bias current/diode (A)	0.11	0.11	0.23	0.26	0.26	0.26	0.26
14.	Power consumption of stage, including regulators (W)	2.8	2.8	5.3	6.0	12.0	24.0	48.0
15.	Efficiency of stage (%)	0.3	3.0	10.9	11.2	10.8	10.8	10.4

Overall efficiency = 10.21/100.9 = 10.1%

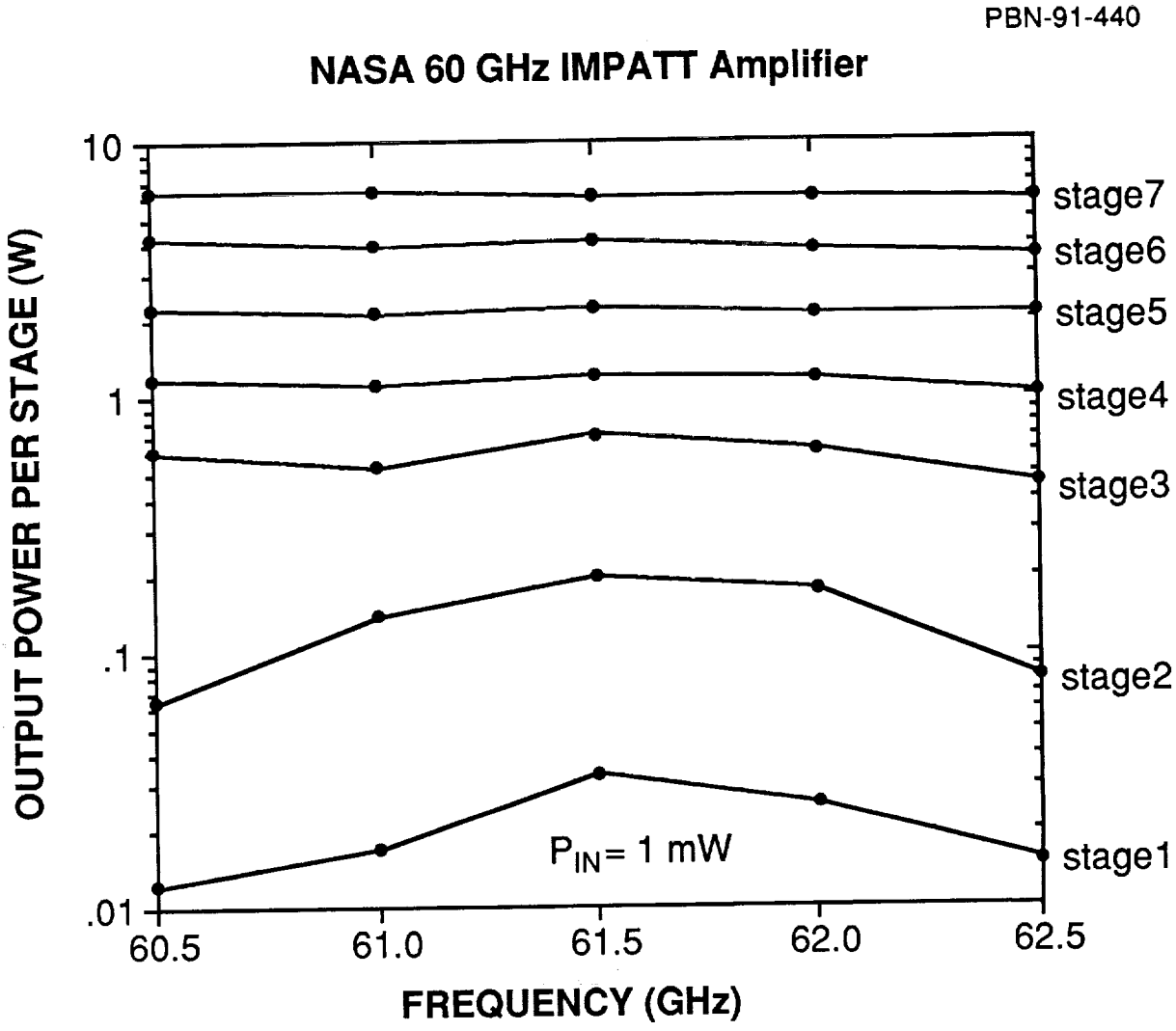

Figure 3-1. Performance of the Seven Stages in the Amplifier.

A new parametric effect was observed in the 8-diode output stage which we did not see in the earlier stages. It is most easily observed when the output power is monitored with a crystal detector and an oscilloscope. The horizontal axis of the oscilloscope is driven by the sweep output of the signal generator so that the output power vs. frequency data of the amplifier is displayed. In the upper half of the frequency band, there are several small, abrupt steps in the data. This effect was not seen in the IMPATT modules when they were tested individually, nor was it observed in the earlier stages. The port match and port isolation of the 8-way combiner were checked in the operating band and found to be excellent. We concluded that the out-of-band port match or port isolation is inadequate to stabilize the the modules from parametric oscillation.

A similar effect was discovered in our 44 GHz amplifiers several years ago. The solution in that application was to add RF absorbing material to the IMPATT modules to suppress the parametric oscillation without absorbing fundamental power. This effect was not discovered in the design phase of this 60 GHz contract because the effect did not occur in the earlier stages. There are several possible approaches for eliminating this problem which we would like to try at some point in the future.

Figure 3-2 shows the output power of the amplifier on a linear scale. The total dc input power is 6.5 amperes at 24 volts, or 156 watts, and the overall efficiency of the amplifier is 4 percent. This result sets the state of the art at V-band, but is it somewhat below the contract goal of 10 percent. The measured performance of all the components was very close to the design values except for the IMPATT diode efficiency. The diodes produce the required output power of 1 watt to meet the amplifier specifications, but extra bias power is needed.

V-band diode development at Raytheon has continued in parallel with this contract, and it will be pursued further in the future. The amplifier requires diodes with 17 percent efficiency to achieve the overall amplifier efficiency goal of 10 percent. We have achieved over 16 percent efficiency from some of our best diodes, but these are uncommon results.

The performance of the 60 GHz IMPATT diodes will improve as these development contracts are continued. The same amplifier design can be retrofitted with improved devices at some time in the future.

3.2 Measurement of Spurious Signals

The output signal of the amplifier was studied with a spectrum analyzer to look for spurious signals. Our spectrum analyzer is a Tektronix 492 with an external V-band mixer, and it has approximately 30 dB of dynamic range. We used this instrument to search for spurious signals as the frequency of the input signal was moved through the operating band. The output spectrum was clean except when one of the output power steps occurred. We explained in Section 3.1 that we believe these steps are due to parametric interaction between the IMPATT modules and the 8-way combiner. The presence of spurious signals in the output supports this explanation of the cause of the power steps.

The spurious signals were out of the range of our frequency meter in the V-band setup, so we cannot be quantitative about their frequency or magnitude. If our 44 GHz amplifier experience is applicable here, then a minor redesign of the IMPATT modules would eliminate all spurious signals.

3.3 Burn-In

The amplifier was operated continuously at full power for two days at the end of the contract. No failures occurred during this period, and the performance did not change. We would have been very surprised if a component had failed since all the IMPATT diodes had been burned-in prior to assembly and the electronic circuit design is quite conservative. We are confident that the amplifier will operate successfully for many years.

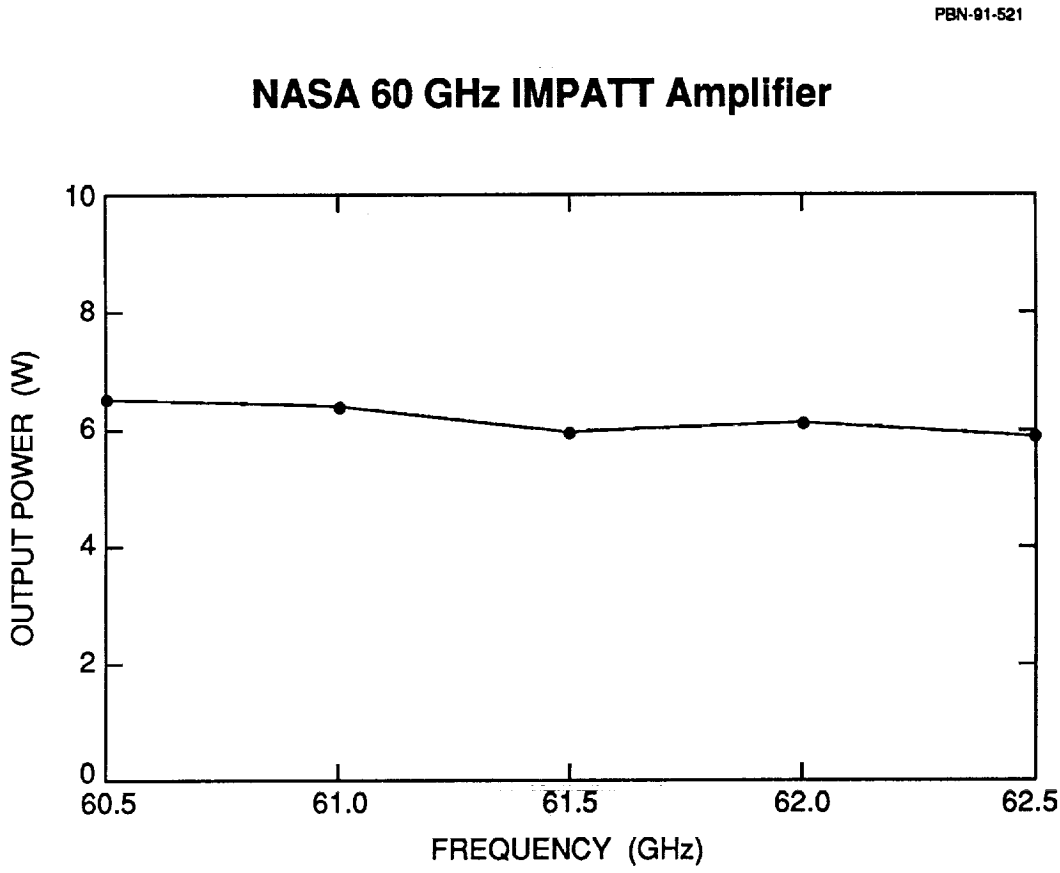

Figure 3-2. Output Power of the Amplifier.

4.0 RELIABILITY PREDICTION

A spacecraft amplifier must be extremely reliable. This was an important consideration throughout the design of this amplifier. Two main approaches were used. First, all the IMPATT diodes and electronic components are highly derated to achieve very low failure rates. Second, most of the components are in the last two stages which have good graceful degradation. In most cases, more than one component failure would be necessary to make the whole amplifier inoperable.

The IMPATT diodes are biased so that the temperature rise from the baseplate to the junction is 170°C or less. If the baseplate temperature in the spacecraft is held to 50°C maximum, the IMPATT diode junction temperature will be no more than 220°C. This is a very conservative temperature, and the life test data in Figure 4-1 shows that the MTTF of each diode is 1×10^7 hours. The associated standard deviation of the data points is between 0.5 and 1.0, indicating a mature diode fabrication process. A graph from Peck and Zierdt [1] converts an MTTF of 1×10^7 and a standard deviation of 1.0 to a failure rate of 1.0 FITs or less. (1 FIT is defined as one failure in 10^9 hours.) The failure rate for all 18 IMPATT diodes in the amplifier is 18 times greater, or 18 FITs maximum.

The failure rate of a similar bias regulator circuit was calculated for another program. At a baseplate temperature of 70°C, the failure rate was 427 FITs, and it was 528 FITs at 86°C. If the maximum baseplate temperature of this amplifier is 50°C, the failure rate of each bias regulator will be about 300 FITs. The failure rate of all the bias regulators will be 18 times

---

1 Peck, Stewart and C.H. Zierdt, Jr., "The Reliability of Semiconductor Devices in the Bell System", Proc. of the IEEE, Vol. 62, No. 2., February 1974.

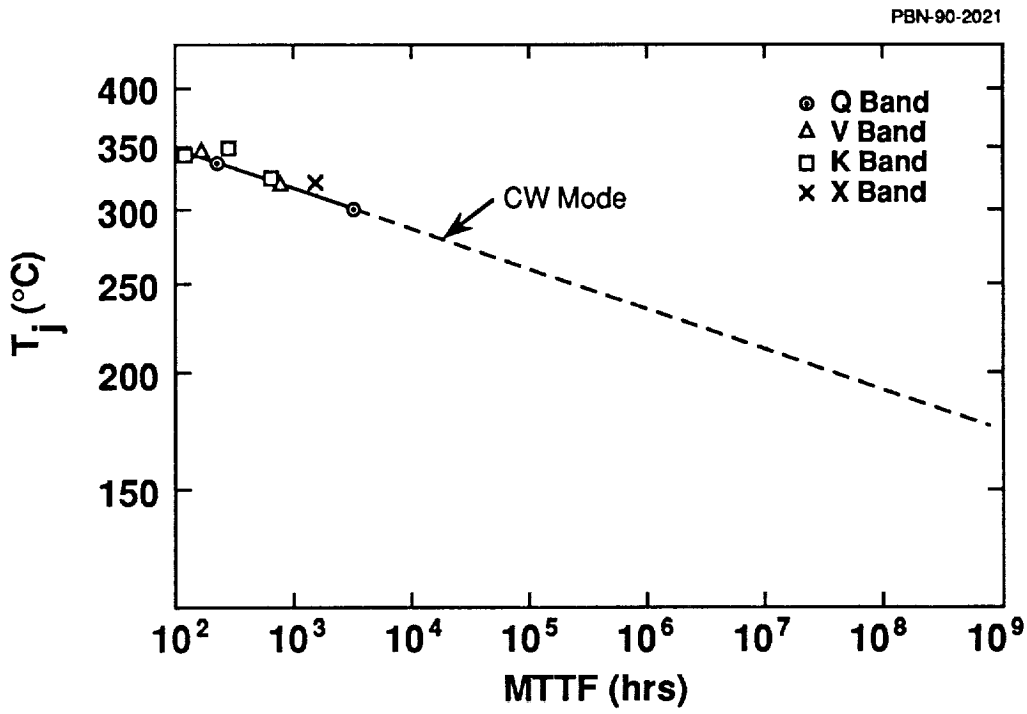

Figure 4-1. Reliability Data of GaAs IMPATT Diodes.

greater. The control circuit has very few components and all are very lightly stressed, so this contribution has been neglected.

Therefore, the total failure rate of the amplifier at 50°C is:

18	FITs	18 IMPATT diodes
+ 5400	FITs	18 bias regulators
5418	FITs	Total

The MTTF of the amplifier is the reciprocal of the total failure rate.

$$MTTF = \frac{1}{5418 \times 10^{-9}} = 2 \times 10^{5} \text{ hours} = 23 \text{ years}$$

This figure exceeds the 10^5 hour requirement of the contract by a factor of two, and does not include the benefit of graceful degradation. Much of the contribution to the failure rate comes from the bias regulator design, and this could be improved when the circuit is redesigned as a hybrid circuit. This would give the amplifier added reliability or allow it to be used at a higher temperature.

5.0 CONCLUSIONS

This program has made a solid contribution to the technology of 60 GHz solid-state amplifiers. Raytheon GaAs IMPATT diodes, having twice the efficiency of the silicon devices that were used in earlier work, were used in this new effort. An elegant building block approach was chosen, and all the required components were developed. A high power automatic network analyzer with specialized software was built so that the operation of the components could be thoroughly understood and optimized.

The final result of the program is an amplifier which generates between 5.9 and 6.5 watts across the 60.5 to 62.5 GHz operating band. The corresponding dc to RF efficiency is 3.8 to 4.2 percent. The components are highly derated, and the expected lifetime before any component fails is 23 years at a baseplate temperature of 50°C. These specifications are very attractive for a spacecraft communications amplifier.

In terms of the program goals, the final amplifier nearly reaches the 10 watt output power goal. Higher power could be achieved by using larger area IMPATT diodes, but this would decrease the efficiency slightly. The overall efficiency goal of 10 percent was a more difficult challenge, and the difference between goal and accomplishment is greater. The primary reason that the amplifier is only 4 percent efficient is that the IMPATT diodes themselves are only 11 percent efficient. Achieving 10 percent overall efficiency requires the IMPATT diodes to have an efficiency of 17 percent or more. We have made some devices with this level of performance, but we have been unable to achieve results like this consistently.

V-band IMPATT diode development will continue and, at some point, this same amplifier or a duplicate could be fitted with improved devices. The overall design philosophy and the design of

the individual passive components were very successful, and the 10 percent amplifier efficiency goal is quite feasible.

It is interesting to compare this work to earlier efforts. The most recent work has been done by TRW (another company) from a NASA contract which ended in 1986. TRW used silicon IMPATT diodes, one-diode amplifier circuits and a 16-way radial line combiner. As a generalization, our gallium arsenide IMPATTs have about the same output power as a silicon IMPATT but with twice the efficiency. The radial line combiner used by TRW had 1.3 dB of attenuation per pass as compared to the 0.35 dB attenuation in our combiner plate. The combiner plate approach also is considerably smaller and it is suitable for conduction cooling in outer space. The TRW amplifier produced 6 watts over a 1 GHz band, with approximately 2 percent overall efficiency. The Raytheon approach has twice the efficiency and bandwidth.

Overall, this contract did much to advance the technology of 60 GHz solid state power amplifiers. New ideas were tried and several major problems were solved. The performance of the final amplifier was markedly superior to earlier work and will be the benchmark for future research.